

DOE/ET/11292--T5

DE81 024381

**Report No. TE4258/4247-149-81**

**DISCLAIMER**

This book was prepared as an account of work sponsored by an agency of the United States Government. Neither the United States Government nor any agency thereof, nor any of their employees, makes any warranty, express or implied, or assumes any legal liability or responsibility for the accuracy, completeness, or usefulness of any information, apparatus, product, or process disclosed, or represents that its use would not infringe privately owned rights. Reference herein to any specific commercial product, process, or service by trade name, trademark, manufacturer, or otherwise does not necessarily constitute or imply its endorsement, recommendation, or favoring by the United States Government or any agency thereof. The views and opinions of authors expressed herein do not necessarily state or reflect those of the United States Government or any agency thereof.

**DOE/JPL  
ADVANCED THERMIONIC  
TECHNOLOGY PROGRAM  
PROGRESS REPORT NO. 45**

**October, November, December  
1980**

*2*  
**DOE Contract DE-AC02-76ET11291  
JPL Contract 955009**

**Prepared by:**  
**Thermo Electron Corporation**  
**101 First Avenue**  
**Waltham, Massachusetts 02254**

*(cp)*  
**DISTRIBUTION OF THIS DOCUMENT IS UNLIMITED**

## **DISCLAIMER**

**This report was prepared as an account of work sponsored by an agency of the United States Government. Neither the United States Government nor any agency Thereof, nor any of their employees, makes any warranty, express or implied, or assumes any legal liability or responsibility for the accuracy, completeness, or usefulness of any information, apparatus, product, or process disclosed, or represents that its use would not infringe privately owned rights. Reference herein to any specific commercial product, process, or service by trade name, trademark, manufacturer, or otherwise does not necessarily constitute or imply its endorsement, recommendation, or favoring by the United States Government or any agency thereof. The views and opinions of authors expressed herein do not necessarily state or reflect those of the United States Government or any agency thereof.**

## **DISCLAIMER**

**Portions of this document may be illegible in electronic image products. Images are produced from the best available original document.**

page blank

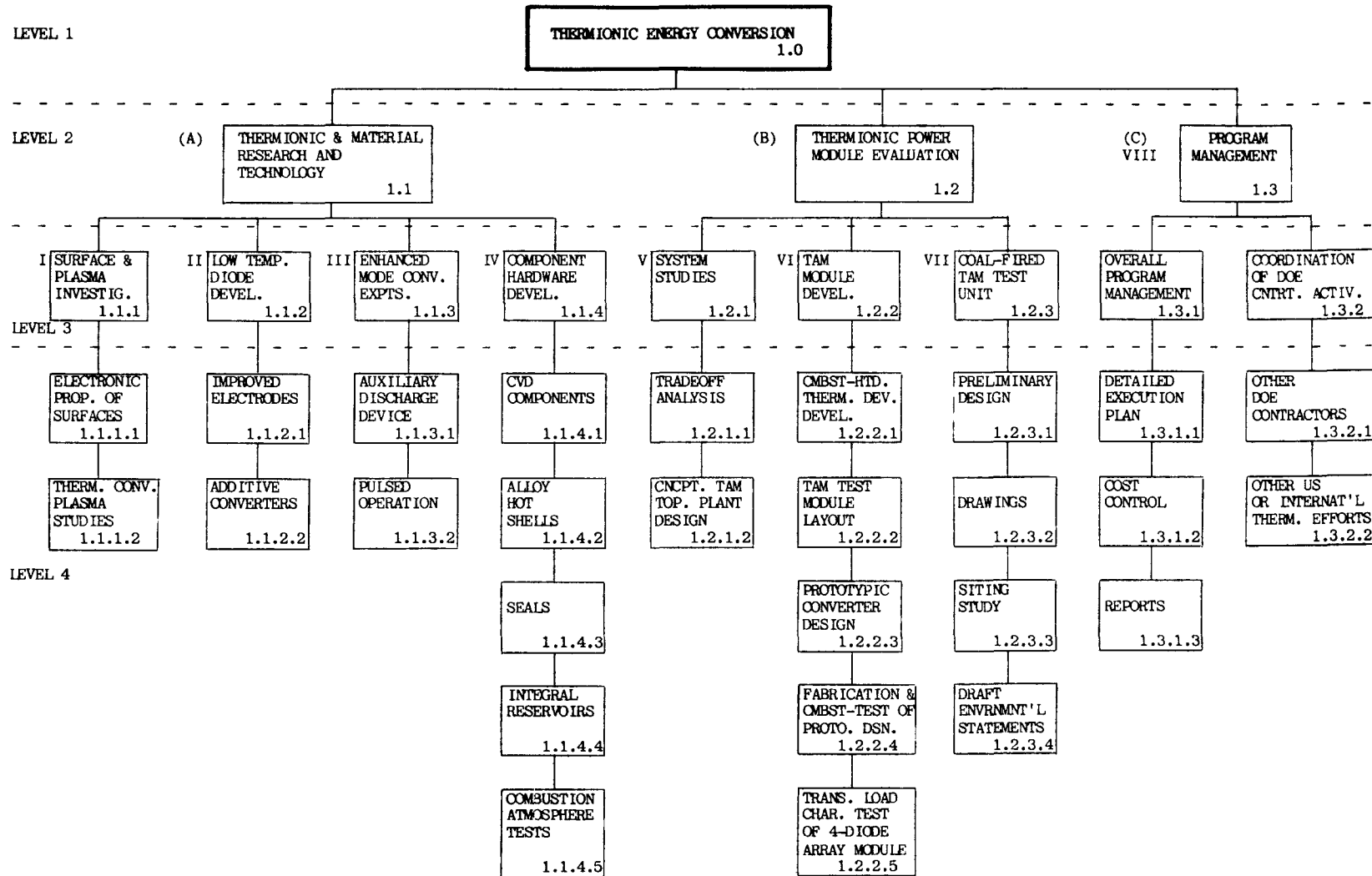
## CONTENTS

INTRODUCTION AND SUMMARY.....	vii
<u>1.0 PART ONE: DOE TASKS.....</u>	1
1.1 THERMIONIC AND MATERIAL RESEARCH AND TECHNOLOGY	1
1.1.1 TASK I. SURFACE AND PLASMA INVESTIGATIONS .....	1
1.1.2 TASK II. LOW-TEMPERATURE CONVERTER DEVELOPMENT	11
A. Converter No. 246: Tungsten Emitter, Nickel Collector, Heat Flux Diode .....	11
1.1.3 TASK III. ENHANCED MODE CONVERTER EXPERIMENTS..	13
1.1.4 TASK IV. COMPONENT HARDWARE DEVELOPMENT.....	14
A. CVD Hot Shell-Emitter Development.....	14
1.2 THERMIONIC POWER MODULE EVALUATION .....	21
1.2.1 TASK V. SYSTEM STUDIES .....	21
1.2.2 TASK VI. TAM MODULE DEVELOPMENT.....	27
A. Converter No. 229: One-Inch Diameter Hemispherical Silicon Carbide Converter (CVD Tungsten As Deposited Emitter, Nickel Collector) .....	27
B. Converter No. 247: Two-Inch Diameter Hemispherical Silicon Carbide Converter (CVD Tungsten as Deposited Emitter, Nickel Collector) .....	28
C. Two-Inch Diameter Torispherical Silicon Carbide Converter .....	28
D. CVD Silicon Carbide Converter Module (Converter Nos. 250, 251, 252, and 253) .....	30
1.2.3 TASK VII. COAL-FIRED TAM TEST UNIT.....	32
<u>2.0 PART TWO: NASA-OAST/JPL TASKS .....</u>	35
2.1 THERMIONIC CONVERTER EVALUATION .....	35
2.1.1 TASK VIII. HIGH-TEMPERATURE CONVERTER EVALUATION.....	35
A. Converter No. 240 (JPL No. 10): Tungsten Emitter, Molybdenum Oxide Collector.....	35
B. Converter No. 242 (JPL No. 9): Tungsten Emitter, Molybdenum Oxide Collector .....	36
C. Converter No. 249 (JPL No. 15): Tungsten Emitter, Molybdenum Oxide Collector .....	37
D. Converter No. 254 (JPL No. 14): Tungsten Emitter, Molybdenum Oxide Collector .....	41
E. Converter No. 256 (JPL No. 16): Tungsten Emitter, Molybdenum Oxide Collector .....	44
F. Converter No. 257 (JPL No. 13): Molybdenum Emitter, Molybdenum Oxide Collector .....	47

page blank

DOE Contract No. EY-76-C-02-3056  
WORK BREAKDOWN STRUCTURE

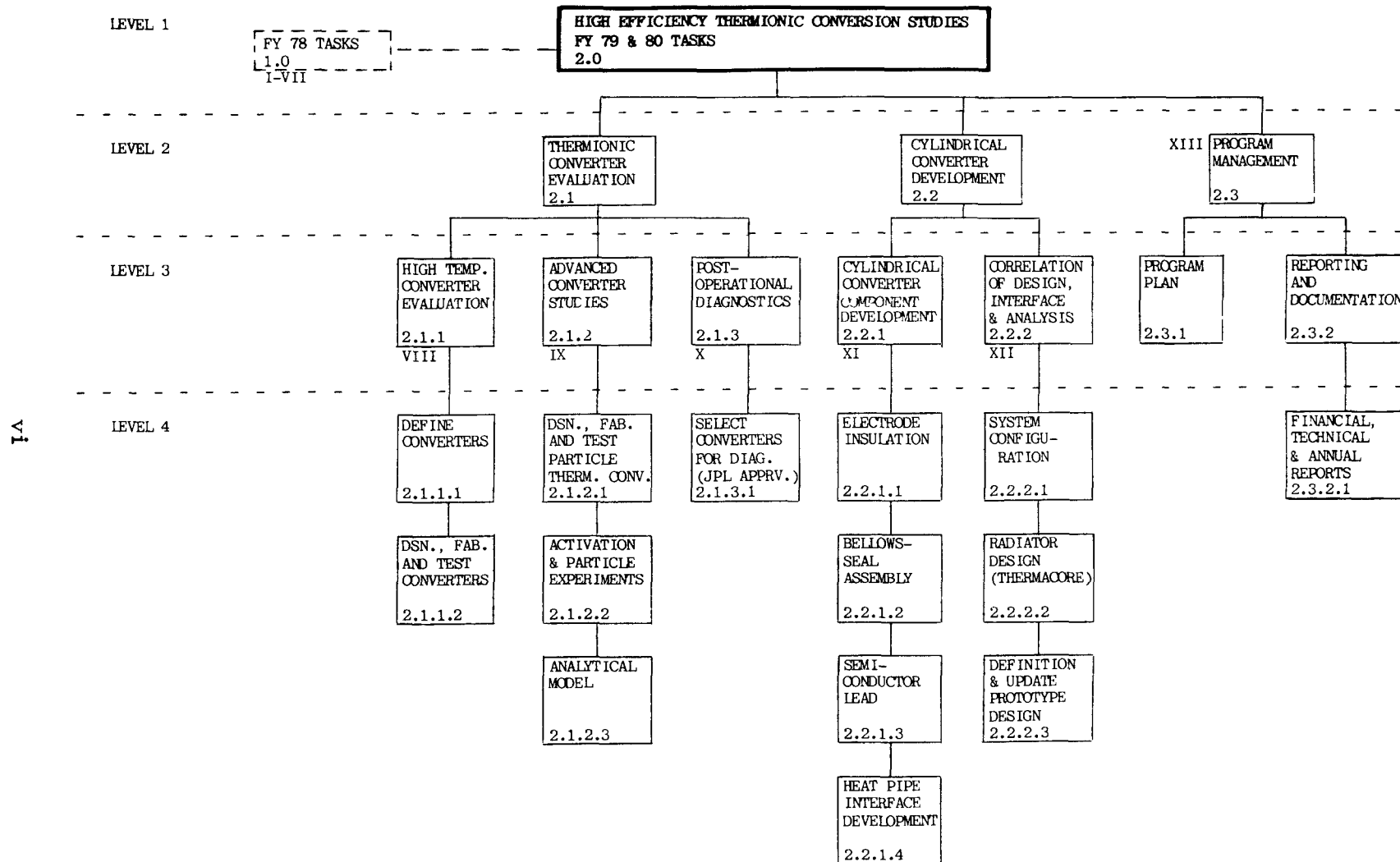
7911-11



Note: Roman Numerals Designate Level at Which Tasks are to be Reported

JPL Contract No. 955009  
WORK BREAKDOWN STRUCTURE

7911-16



Note Roman Numerals Designate Level at which Tasks are to be Reported.

## INTRODUCTION AND SUMMARY

The Advanced Thermionic Technology Program at Thermo Electron Corporation is sponsored by the Department of Energy (DOE) and the National Aeronautics and Space Administration (NASA) via the Jet Propulsion Laboratory (JPL).

The primary long-term goal of the DOE effort is to improve TEC performance to the level that thermionic topping of fossil fuel powerplants becomes technically possible and economically attractive. An intermediate goal is to demonstrate an in-boiler thermionic module in the early 1980's. A short-term goal is the demonstration of the reliability of thermionic operation in a combustion environment.

The focus of the JPL program is to develop thermionic conversion technology appropriate for nuclear electric propulsion (NEP) missions. These missions require operation at collector temperatures that are substantially higher than those associated with terrestrial applications.

The DOE and JPL tasks for developing thermionic energy conversion (TEC) are complementary and synergistic. Converter performance improvement is an area in which one agency's program supports the effort of the other.

This report covers progress made during the three-month period from October through December 1980. During this period, significant accomplishments include:

**DOE PROGRAM**

- Continuing stable output from the combustion life test of the one-inch diameter hemispherical silicon carbide diode (Converter No. 239) at an emitter temperature of 1730 K for a period of over 4200 hours.
- Construction of four diode module completed.
- Favorable results obtained from TAM combustor-gas turbine system analyses. A summary briefing on this study was presented at DOE (Germantown) on December 11.
- Obtained a FERP work function of 2.3 eV with the W(100)-O-Zr-C electrode.

**JPL PROGRAM**

- The average minimum barrier index of the last six research diodes built with sublimed molybdenum oxide collectors was 2.0 eV.

## 1.0 PART ONE: DOE TASKS

### 1.1 THERMIONIC AND MATERIAL RESEARCH AND TECHNOLOGY

#### 1.1.1 TASK I. SURFACE AND PLASMA INVESTIGATIONS

The objective of this task is to support the development of thermionic energy converters by providing experimental data and analyses relating to plasma characteristics and electrode properties

The Zr-O-W(100) emitter has a work function of 2.7 eV and is stable at high temperatures. The addition of carbon is believed to lower this work function further. During this reporting period, the coadsorption of carbon monoxide (CO) and zirconium (Zr) onto W(100) was investigated with emphasis on the work function change. Three methods of exposing the W(100) surface to CO and Zr were employed.

In the first method, Zr was deposited first onto clean W(100). The ratios of zirconium 92 eV to tungsten 169 eV Auger peak-peak heights for three runs were 0.51, 1.33 and 2.45. The sample was then heated in  $10^{-7}$  torr CO for 10 minutes with the sample held at 1500 K

followed by a one minute vacuum anneal to 1600 - 1700 K.

The resultant FERP work functions after the anneal were 2.56, 2.60, and 2.53 eV. Appreciable carbon was present on the surface after the anneal, indicating that carbon can lower the work function below the 2.7 eV value obtained for Zr-O-W(100). The work function after annealing is surprising since it is relatively independent of the initial dose over the range of Zr concentration studied.

In the second method, the cleaned W(100) crystal was held at 1200 K and exposed to  $60 \times 10^{-6}$  torr-sec (60L) of CO. The crystal was then exposed to Zr in vacuum and heated for one minute at progressively higher annealing temperatures (see Figure 1). The Auger scans were taken at room temperature, and the zirconium 92 eV peak was used in all Auger measurements for this and succeeding graphs. The work function gradually decreases to a minimum of 2.38 eV as the anneal temperature varies from 1200 - 1700 K. The elemental surface concentrations change little during these heatings, suggesting that an activation energy must be exceeded in order to reach the minimum work function. The work function rises to 3.05 eV after the 1800 K anneal, and the carbon and oxygen concentrations decrease markedly, apparently due to CO desorption.

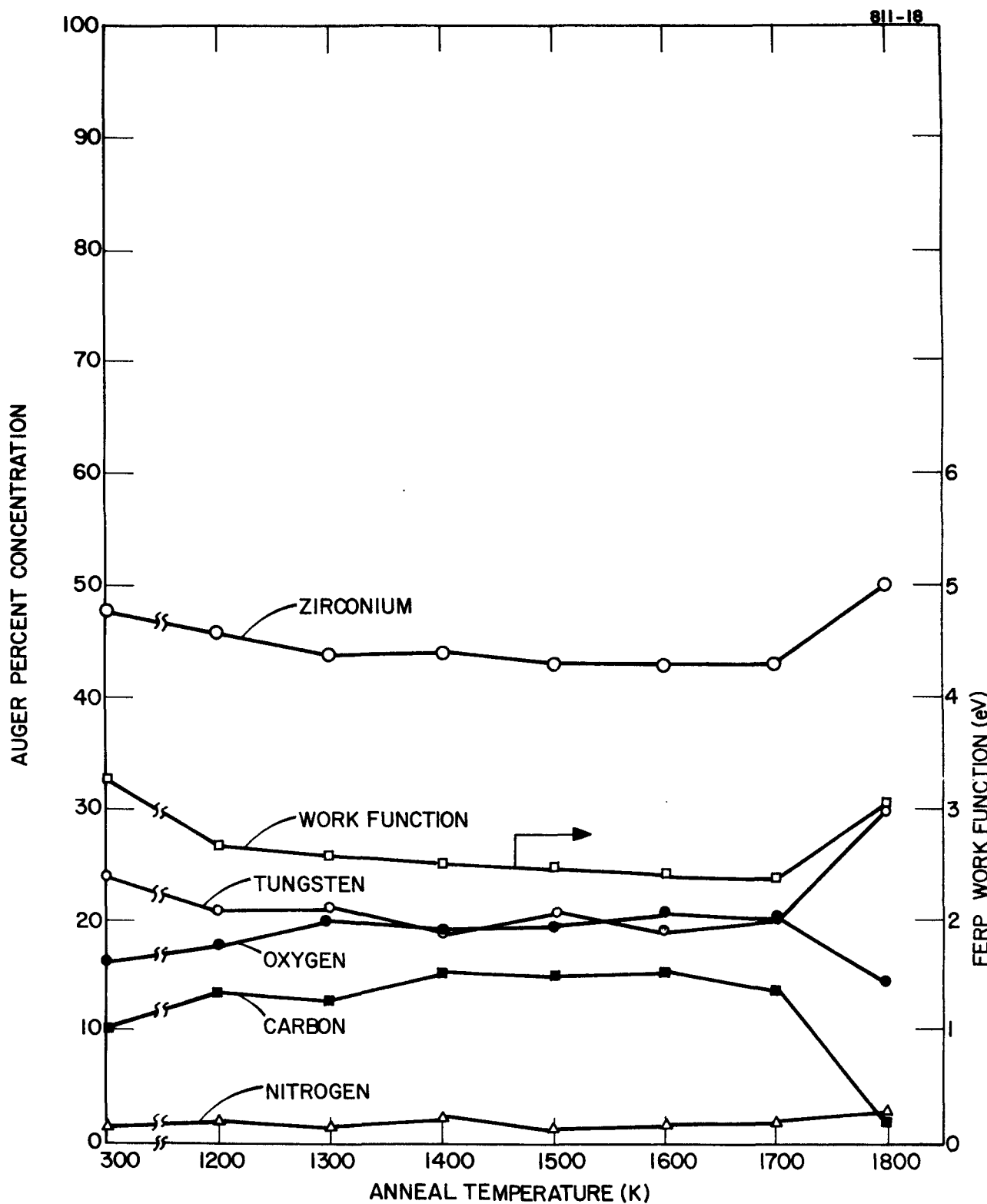


Figure 1. Auger Percent Concentration and Work Function Versus Anneal Temperature for CO and Zr Deposited on W(100).

In the third method, CO was adsorbed first (as in the second method), but with the cleaned crystal at room temperature. The exposure providing saturated CO coverage was determined to be approximately 120 L by plotting C/W and O/W Auger ratios as a function of CO exposure (see Figure 2). The fact that the C/W ratio saturates much sooner than the O/W signal is not understood, but may be due to a rearrangement of CO molecules on the surface during the dosing. [The gas purity was monitored with a mass spectrometer, and beam current was held at 1  $\mu$ A to minimize beam effects.]

The 120 L CO exposure with the crystal at room temperature was followed by a zirconium dose. The work function versus  $Zr_{92}/W_{169}$  Auger ratio is shown in Figure 3. The work function decreases from 5.3 eV to 3.1 eV.

For each  $Zr_{92}/W_{169}$  ratio in Figure 3, the crystal was then annealed in vacuum at 1700 K for one minute. The FERP work function after anneal versus  $Zr_{92}/W_{169}$  ratio is shown in Figure 4. The  $Zr_{92}/W_{169}$  ratio for both Figures 3 and 4 was measured before annealing, and for each data point in Figure 4, the crystal was flashed

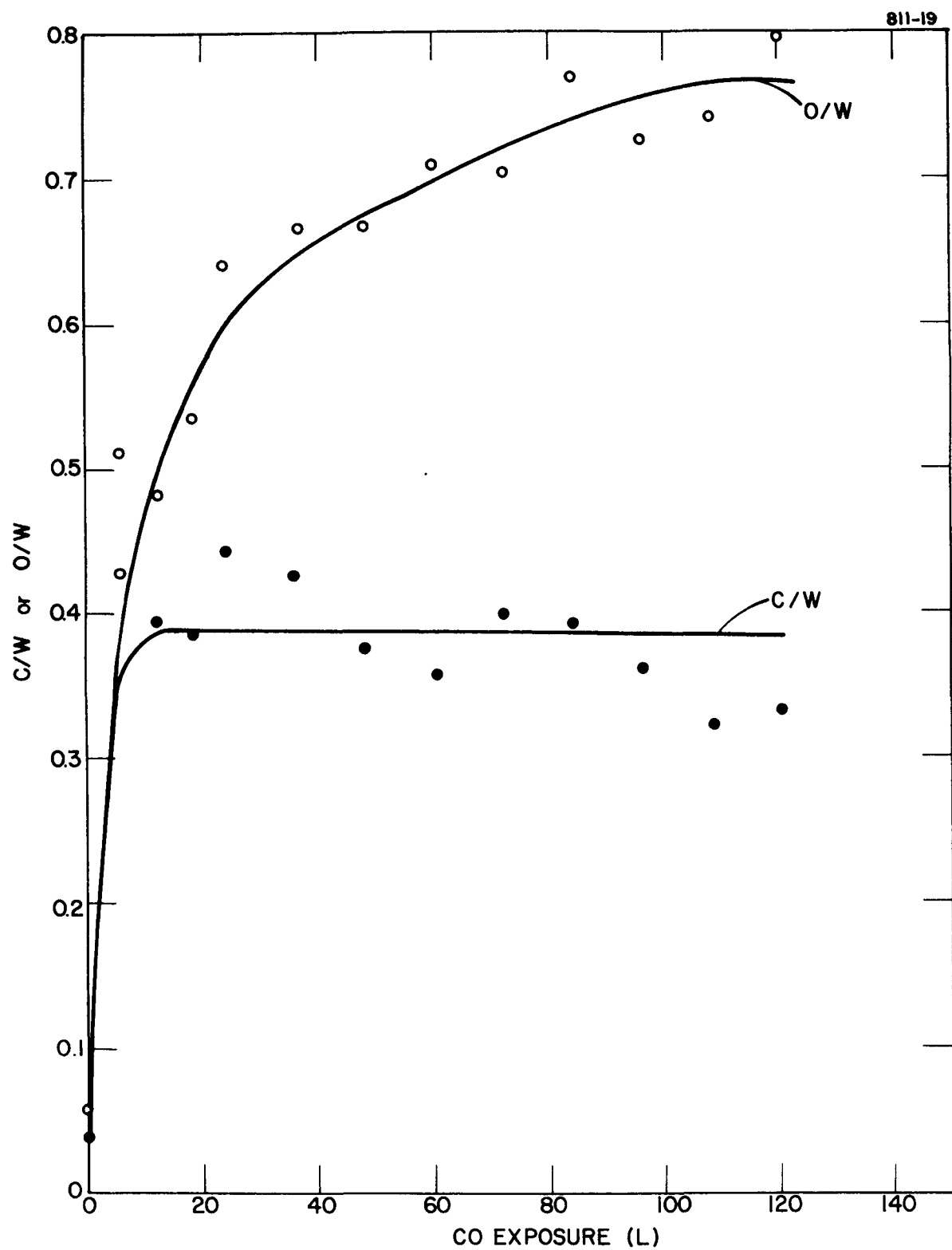


Figure 2. Oxygen/Tungsten and Carbon/Tungsten Ratios Versus CO Exposure

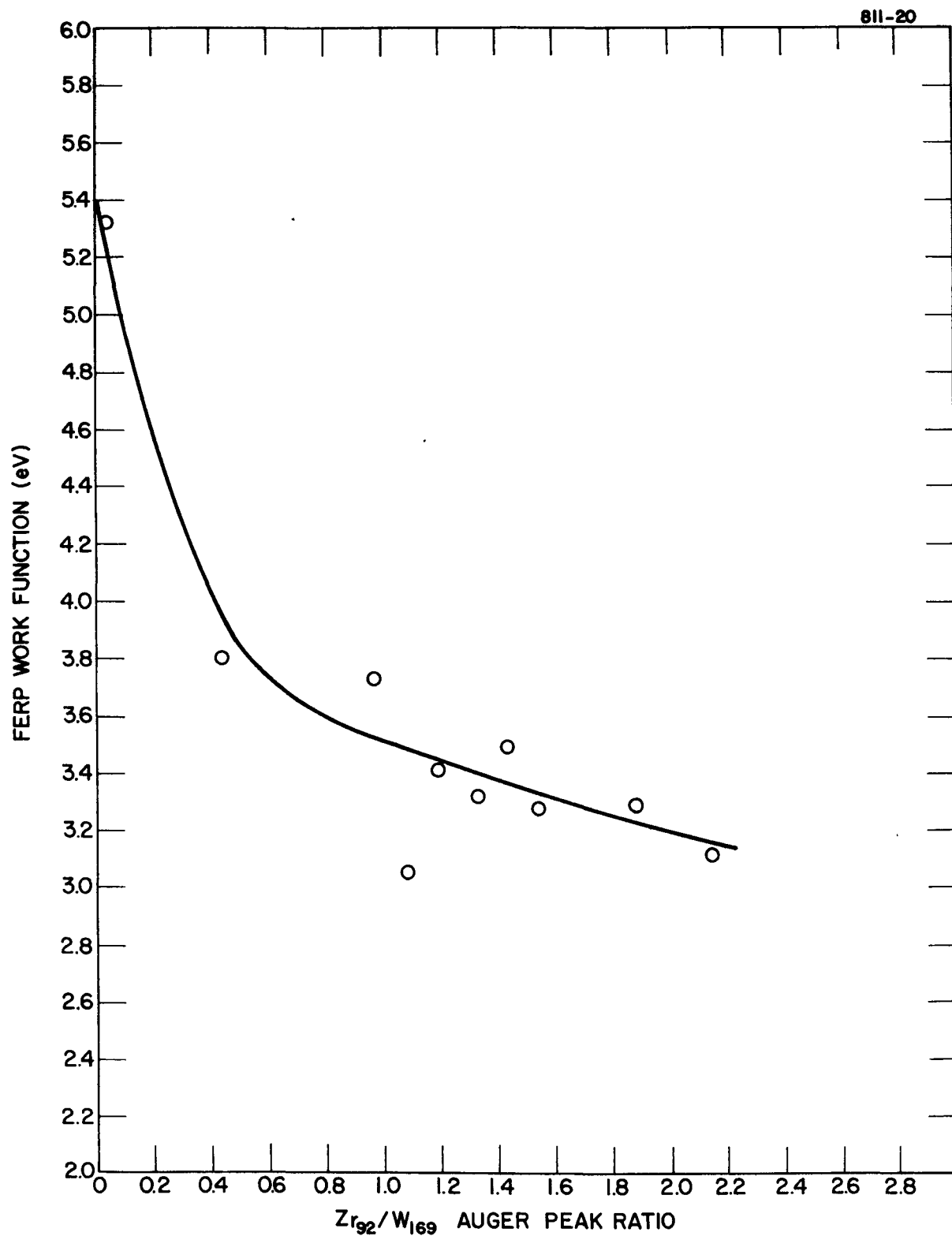


Figure 3. FERP Work Function Before Anneal Versus  $Zr_{92}/W_{169}$  Auger Peak Ratio for CO and Zr Deposited on W(100)

8012-63

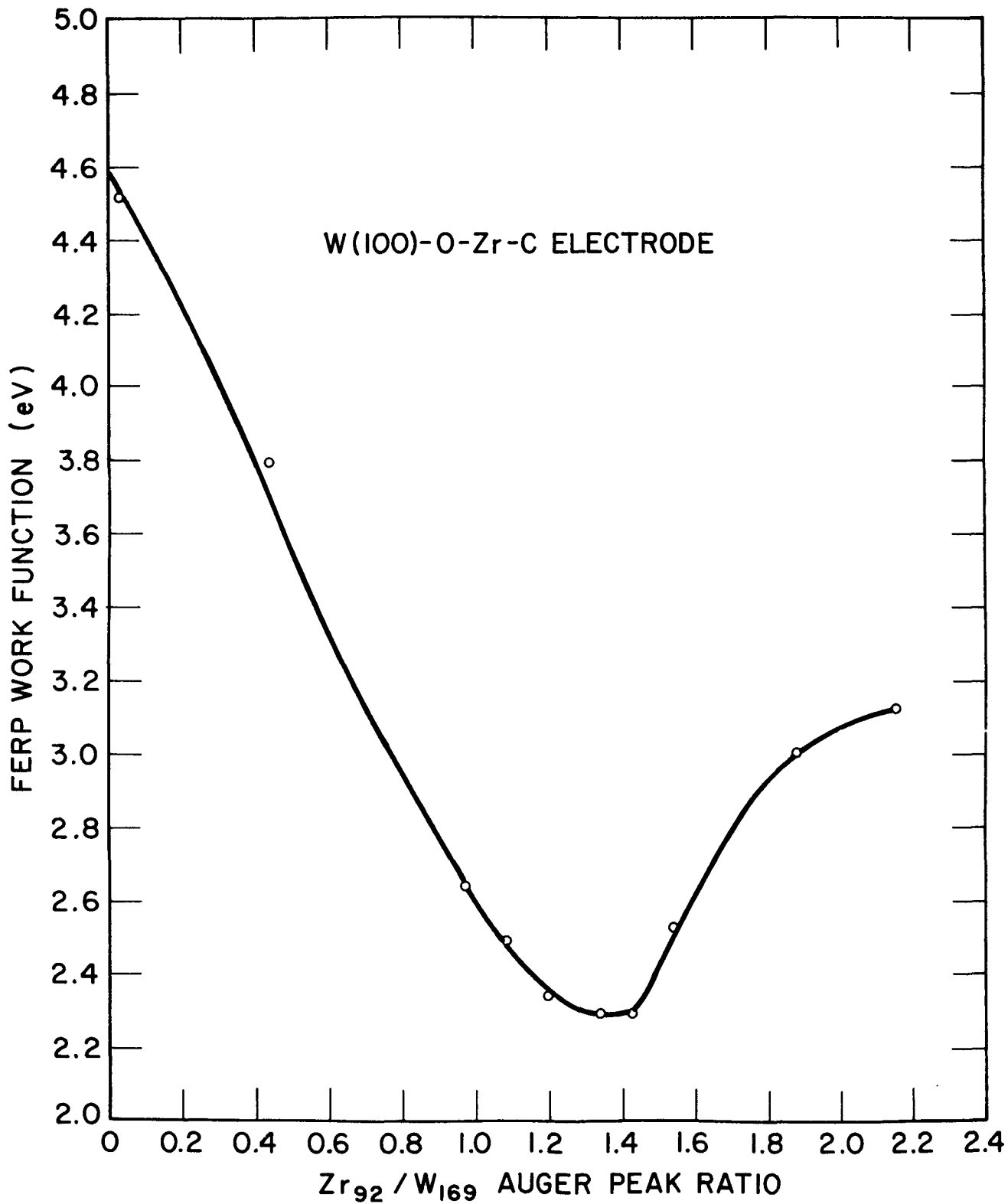


Figure 4. Work Function After Anneal Versus Zr<sub>92</sub>/W<sub>169</sub> Auger Peak Ratio for CO and Zr Deposited on W(100)

to 2400 K, exposed to CO, exposed to Zr, and annealed to 1700 K. The minimum work function obtained is 2.29 eV, which is 0.4 eV lower than the work function obtained for Zr-O-W(100) without carbon. The work function is strongly dependent on the  $Zr_{92}/W_{169}$  ratio, and a value for  $Zr_{92}/W_{169}$  between 1.30 and 1.45 is necessary to obtain the minimum work function.

The work functions obtained in Figure 4 can be related to the elemental surface concentrations. The percent concentrations after annealing of Zr, Zr+O and Zr+O+C, versus work function are shown in Figure 5. The graph shows that maximizing the Zr or Zr+O concentrations does not minimize the work function, whereas maximizing the Zr+O+C concentrations does minimize the work function.

The primary conclusions from this study are 1) a surface with a work function of 2.3 eV can be obtained by coadsorption of CO and Zr onto W(100) followed by a vacuum anneal, 2) the order of deposition is important (CO must be deposited before the Zr in order to obtain the lowest work functions), and 3) maximizing the percent concentration of Zr+O+C results in the minimum work function.

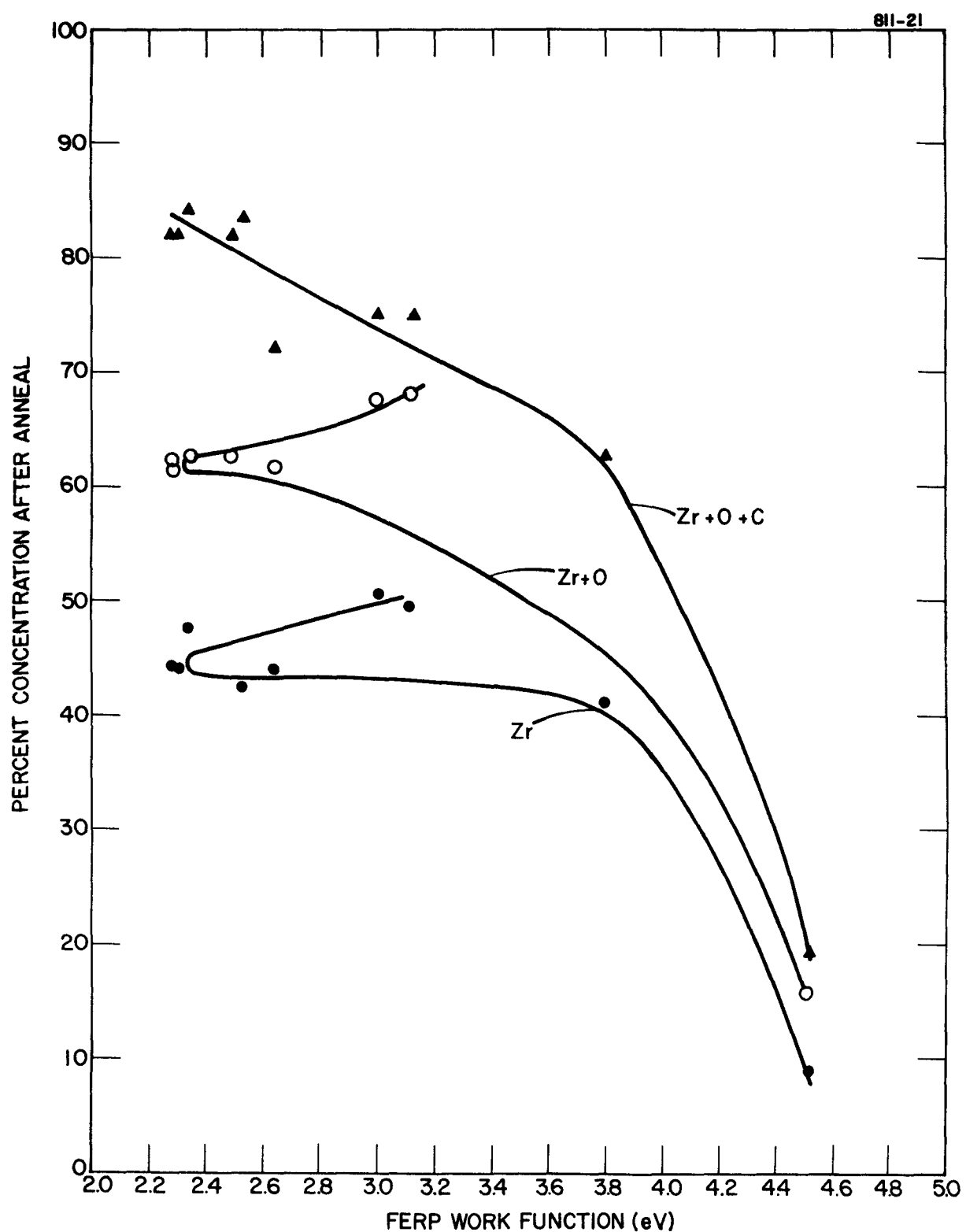


Figure 5. Percent Concentration of Zr, Zr+O, and Zr+O+C After Anneal Versus Work Function for CO and Zr Deposited on W(100)

Tests of the stability of this low work function surface under extended heating and adsorption of background gases are in progress.

### 1.1.2 TASK II. LOW-TEMPERATURE CONVERTER DEVELOPMENT

The objective of this task is to develop thermionic diodes with improved performance at low collector temperatures (i.e., 500-900 K). Converter characteristics will be measured as a function of emitter temperature, collector temperature, cesium pressure, interelectrode spacing and, if applicable, additive gas pressure.

#### A. Converter No. 246: Tungsten Emitter, Nickel Collector, Heat Flux Diode

The collector work function was measured by the retarding plot method. The minimum work function of 1.54 eV is consistent with other measurements made on nickel in the variable-spaced research converter. The collector work function versus the ratio  $T_C/T_R$  is presented in Figure 6.

Prior to collector heat flux measurements, the diode will be characterized at higher emitter temperatures, and the collector work function measurement will be repeated at various electrode temperatures.

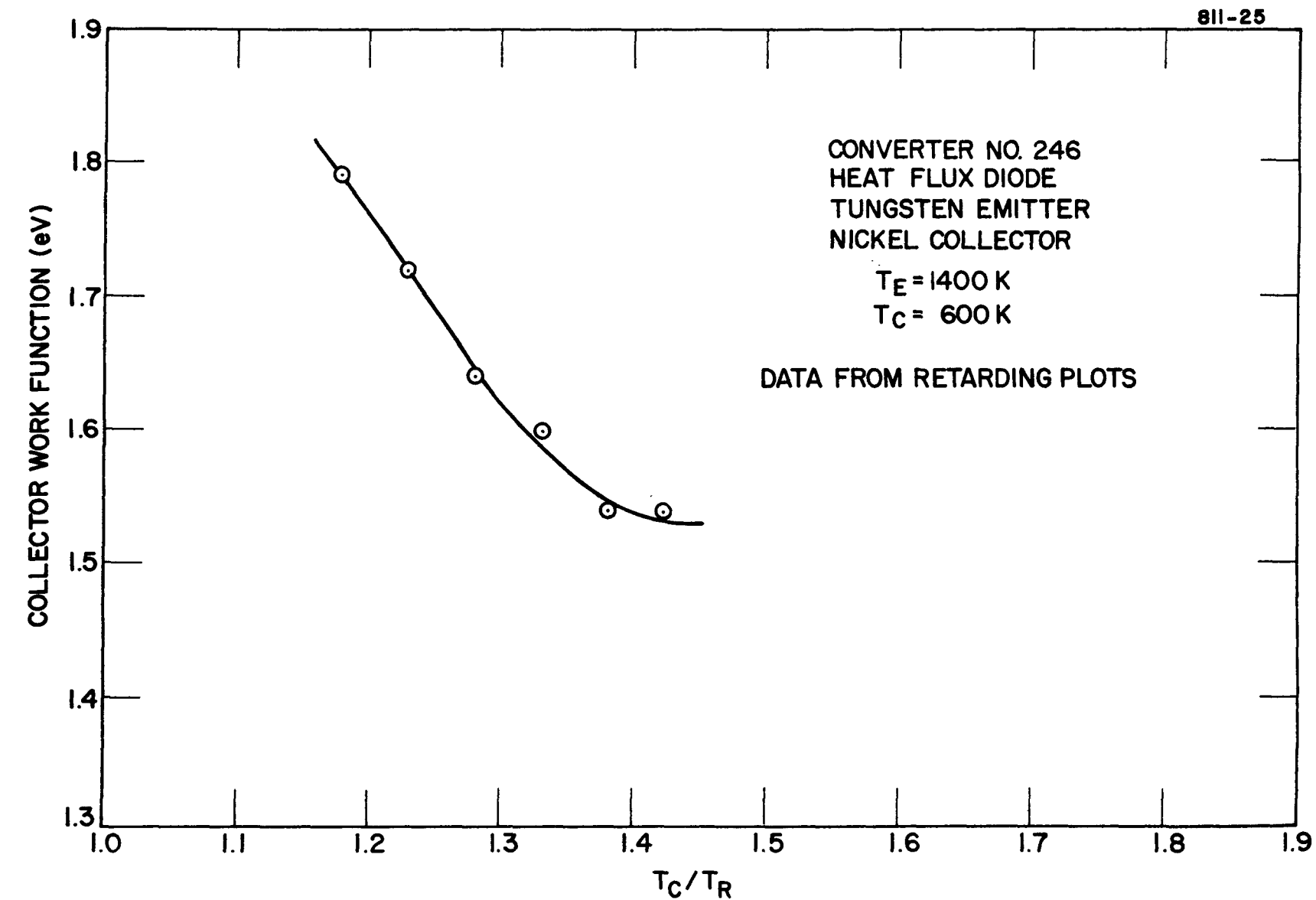


Figure 6. Collector Work Function Versus  $T_C/T_R$  for Converter No. 246

### 1.1.3 TASK III. ENHANCED MODE CONVERTER EXPERIMENTS

The objective of this task is to formulate and evaluate thermionic converter configurations which have the potential of operating more efficiently than the conventional ignited mode diode. In the ignited mode, the mechanism for supplying the ions for space charge neutralization is not efficient. Other techniques which allow the converter to operate in the unignited mode (e.g., those utilizing auxiliary discharge regions and surface contact ionization electrodes) should be more efficient in producing ions and, hence, more efficient in converting heat into electricity. Close-spaced devices that do not require ions should also be more efficient than ignited mode diodes. In the ignited mode, structured electrodes offer the possibility of significantly reducing the plasma losses. Several types of enhanced mode converters will be investigated experimentally.

No effort was expended on this task during this reporting period.

#### 1.1.4 TASK IV. COMPONENT HARDWARE DEVELOPMENT

The objective of this task is to develop converter hardware suitable for operation in a combustion atmosphere such as would be encountered in a thermionic-topped fossil fuel powerplant. Although the effort includes considerable materials evaluation, the focus is on the fabrication and testing of hot shell - emitter subassemblies utilizing chemical vapor deposition (CVD) of composite silicon carbide-graphite-tungsten structures.

##### A. CVD Hot Shell-Emitter Development

###### 1) Hot Shell Fabrication

During this reporting period, four leaktight torispherical hot shells were fabricated. The approximate dimensions are two inches in diameter by two inches long, as shown in Figure 7. The tungsten deposit on these shells was very uniform. All shells had a thickness profile of  $\pm 0.002$  inches along the torispherical end. The silicon carbide deposit was different in appearance from the previous deposits on hemispherical shells. A shiny ring was located on the nose of all the shells. This ring was approximately one to one and a

8II-17

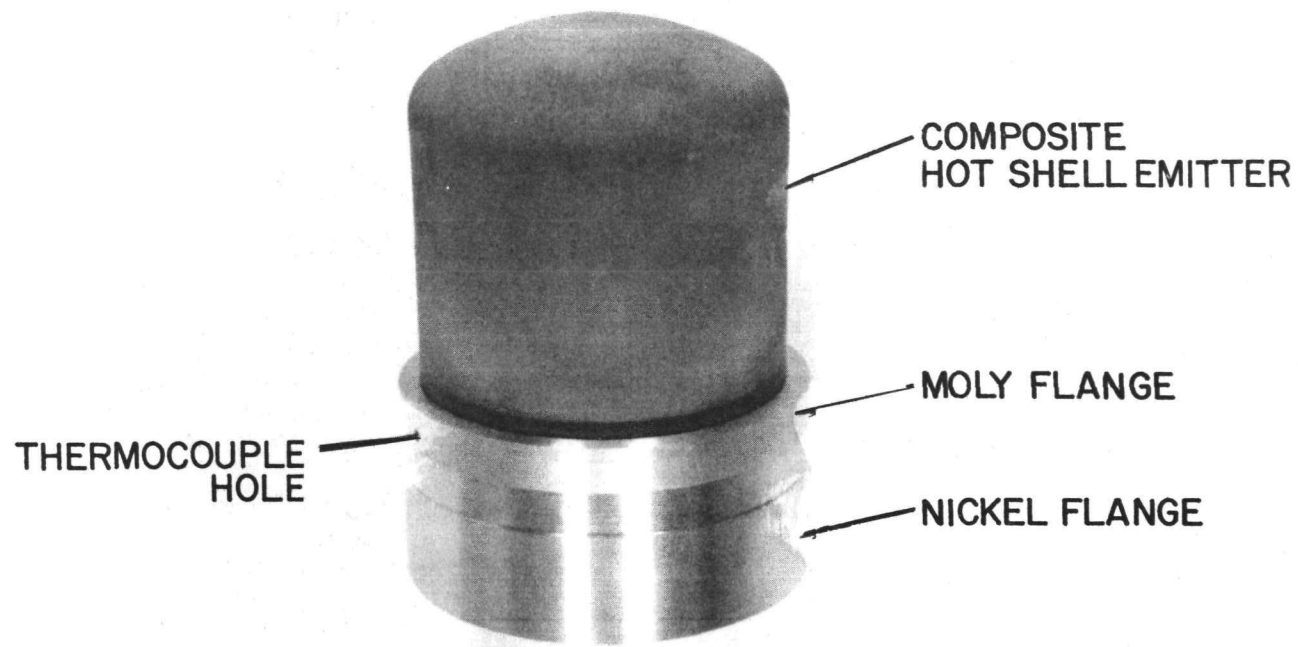


Figure 7. Two-Inch Torispherical Hot Shell-Emitter and Flange

half inches in diameter and centered on the dome. Several substrate temperature profiles were used during deposition, but a shiny ring always resulted on the nose. Further experiments will continue in this area in order to eliminate this shiny deposit.

2) Composite Hot Shell-Emitter Flange Life Tests

Testing at operating temperatures continued on two-inch hot shell-emitter and flange structures. These tests are summarized in Table I.

One of the four leaktight torispherical shells (Shell No. 109) was brazed to a molybdenum flange and coated with Cermetal 487. This shell was two inches in diameter and two inches long. It operated for 1100 hours at 1580 K on the emitter and 850 K at the flange. An important result of this test was that the emitter temperature varied only  $\pm$  15 K over the complete dome area. The emitter temperature is hottest at the center and coolest at the edge. The emitter temperature for a two-inch diameter hemispherical shell varies  $\pm$  35 K over the area of the dome. Also, the torispherical shell was

TABLE I  
HOT SHELL-EMITTER-FLANGE STRUCTURE TESTS

DESCRIPTION (NUMBER)	NUMBER OF HOURS	TEMPERATURE OF DOME OF SHELL (K)	TEMPERATURE OF FLANGE (K)	TEMPERATURE CYCLES	COMMENTS
1" DIAMETER 4" LONG HEMISPERICAL HOT SHELL (101)	110	1925	675 K	9	Black residue on flange. No cracking of structure. Tungsten leaktight.
2" DIAMETER 4" LONG HEMISPERICAL HOT SHELL (102)	70	1655	675	1	Black residue on flange. SiC cracked and braze swelled.
1" DIAMETER 4" LONG HEMISPERICAL HOT SHELL (103)	80	1925	850	13	Flange coated with Cermetal 487. SiC cracked at dome. No black residue.
2" DIAMETER 3" LONG HEMISPERICAL HOT SHELL (104)	2480	1600	850	10	Flange coated with Cermetal 487. SiC leaked 1" from nose. Braze area remained leaktight.
1" DIAMETER 4" LONG HEMISPERICAL HOT SHELL (105)	70	1875	675	20	Leaktight after 70 hours at 1875 K.
	4	1875	675	150	Thermal cycles from 900 K to dome temp.
	2	2025	700	100	Heating and cooling period 30 seconds.
2" DIAMETER 3" LONG HEMISPERICAL HOT SHELL (107)	1700	1600	850	8	Test Continuing
2" DIAMETER 3" LONG HEMISPERICAL HOT SHELL (108)	230	1600	850	3	SiC Cracked one inch from nose.

TABLE I (Continued)

## HOT SHELL-EMITTER-FLANGE STRUCTURE TESTS

DESCRIPTION (NUMBER)	NUMBER OF HOURS	TEMPERATURE OF DOME OF SHELL (K)	TEMPERATURE OF FLANGE (K)	TEMPERATURE CYCLES	COMMENTS
2" DIAMETER 2" LONG TORISPHERICAL HOT SHELL- (109)	1100	1550	850	4	Leak at Braze Joint.
2" DIAMETER 3" LONG HEMISPHERICAL HOT SHELL (110)	192	1600	850	3	Test Continuing.
2" DIAMETER 3" LONG HEMISPHERICAL HOT SHELL (111)	10	1500	800	1	Test Continuing.

an inch shorter (2 inches long) than the hemispherical shells (3 inches long). This shortened version eliminates one inch of tungsten which will reduce the cost of materials by about 25 percent. This torispherical shell developed a leak at the braze area. It will be sectioned and analyzed at its failure point.

Shell No. 107 continued to operate at 1600 K at the nose. The nodules of silicon carbide have remained the same in appearance during the entire test.

A leak developed in the silicon carbide of Shell No. 108, one inch up from the flange. This part of the shell operated at approximately 1000 K and was quite close to the insulating material. An examination of this insulator surrounding the shell indicated that it had come in contact with the silicon carbide. The silicon carbide thickness at this position is approximately 0.005 inch thick. It seems likely that a reaction between the silicon carbide and the insulating material caused the leak.

Tests of Shell Nos. 110 and 111 have begun. Both shells and flanges were coated with Cermetal 487. When these shells have operated and remained stable for at least 200 hours, the flange temperature will be raised to 950 K for life testing.

Shell No. 107 continued to operate at 1600 K at the nose. The nodules of silicon carbide have remained the same in appearance during the entire test.

Shell No. 108 developed a leak in the silicon carbide, one inch up from the flange. This part of the shell operated at approximately 1000 K and was quite close to the insulating material. An examination of this material revealed that it had crumbled and come into contact with the silicon carbide shell. The silicon carbide thickness at this position is approximately 0.005-inch thick. There may have been a reaction between the silicon carbide and the insulating material to cause this leak.

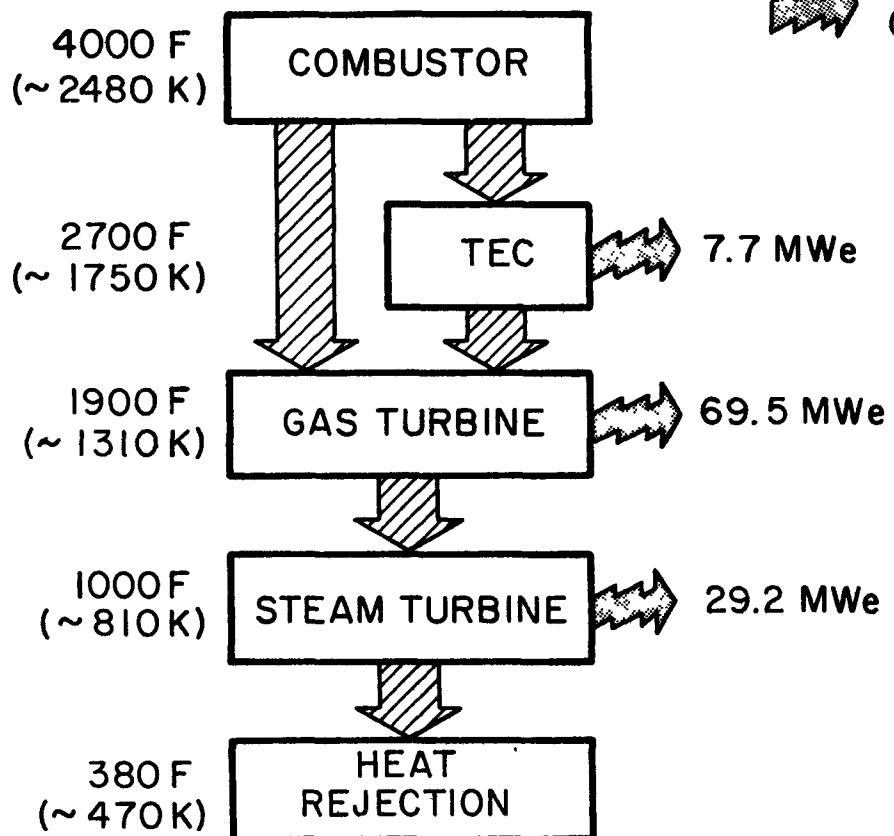
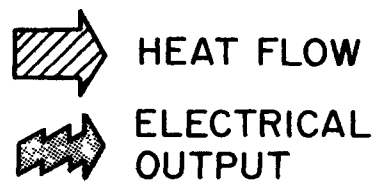
## **1.2 THERMIONIC POWER MODULE EVALUATION**

### **1.2.1 TASK V. SYSTEM STUDIES**

The objective of the system studies task is to identify the design approaches to integrate thermionic energy converters into fossil fuel applications in the most cost-effective manner. The results of these studies will help orient the design of the thermionic array module (TAM) being developed in Task VI.

On December 11, a summary briefing on TAM Combustor Gas Turbine Systems was presented at Germantown, MD. Representatives of Brown Boveri Turbomachinery (BBT) Stone and Webster Engineering and Thermo Electron participated in this briefing. A block diagram of a TAM combustor coupled to a combined cycle is given in Figure 8. This study indicates that the system incremental costs are as favorable as those of the preliminary investigation, which was based on a highly idealized model.

A combined gas and steam turbine system built by BBT was chosen as the reference plant. This system uses a single combustor which can fire medium Btu gas. The nominal output of the gas and steam turbines were 70 MW and 30 MW, respectively. The fuel was assumed to be

LEGEND:

**PLANT EFFICIENCY - 44.6 %**

Figure 8. Block Diagram of TAM Combustor Combined Cycle System

coal-derived medium Btu gas obtained from an oxygen blown entrained gasifier (e.g., the Cool Water Plant), which produces pressurized gas at 480 K (400 F) with an approximate composition of 52% CO and 36% H<sub>2</sub>.

The TAM thermionic converters line the walls of the gas turbine combustor. The design concept of the TAM combustor is illustrated in Figure 9. The thermionic converters produce electricity, and the rejected heat is used to preheat the combustion air. In order to minimize the production of oxides of nitrogen (NOX), two stages of combustion are used. The first stage burns rich. The combustion gases in this stage are cooled by giving up heat to the emitters of the thermionic converters. Preliminary equilibrium calculations indicate that the NOX level resulting from the rapid quenching of the rich mixture may be environmentally acceptable. A reduction of NOX already formed could be achieved by ammonia injection into the rich mixture. A fraction of the air (which bypassed the combustor) is reintroduced to complete the combustion at a lower temperature, and the mixed gases flow to the turbine. The exhaust gases from the turbine flow to the heat-recovery boilers of the bottoming steam cycle.

8012-7

24

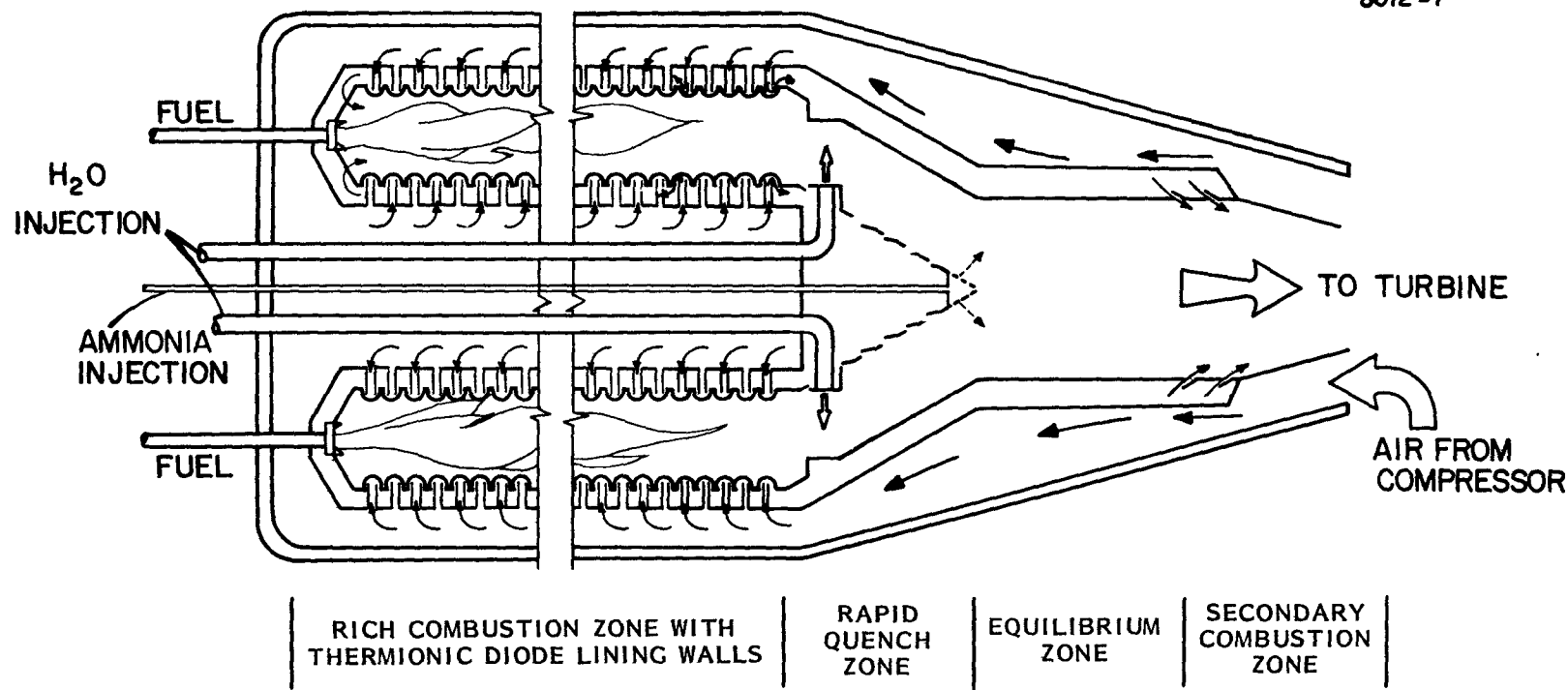


Figure 9. TAM Combustor Design Concept

The gas and steam turbine performances were based on data from BBT. The performance of the (TAM) thermionic converters for the reference case was based on measurements of converters fired with a natural gas flame. One converter, at an emitter temperature of 1630 K, has operated for 5100 hours in a continuing test.

The cost of the base plant was obtained from prices quoted for similar plants by BBT. The cost of the thermionic converter was estimated based on vendor quotations for commercial quantities.

The results indicate that for a 99 MW combined cycle plant, TAM topping reproduces an additional 8 MW at a very favorable heat rate of 3800 Btu/kWh. The incremental busbar cost of producing the thermionic power is 60 percent that of the untopped base plant.

The primary conclusions for this more detailed systems studies are:

- TAM Combustor Topped Gas Turbine Systems:
  - Have attractive incremental costs per kilowatt ( $\sim 500 \text{ \$/kW}$ )
  - Lower cost of electricity for fuel gas cost  $> 1.50 \text{ \$/10}^6 \text{ Btu}$

- Integrated gasifier systems have worthwhile savings
- Thermionic cost and performance is not sensitive to system parameters
- NOX suppression is practical using two stage combustion in conjunction with noncatalytic ammonia injection
- TAM combustor system has high credibility based on operation of CVD silicon carbide thermionic converters at design temperatures for over 15,000 diode hours in a combustion atmosphere
- TAM combustor topping complements high-temperature gas turbine program

Stone and Webster Engineering Corporation is continuing the preparation of a topical report on the application of thermionic topping to combined gas and steam turbine powerplants, as well as on powerplants integrated with a coal gasifier.

### 1.2.2 TASK VI. TAM MODULE DEVELOPMENT

The objective of this task is to develop combustion-heated TAM thermionic converters, individually and in small arrays, which are prototypic for topping a central-station powerplant. Devices with both alloy and silicon carbide hot shells will be made and tested. In order to define the transient thermal and electrical characteristics of a TAM, a four-converter array will be constructed and tested.

#### A. Converter No. 229: One-Inch Diameter Hemispherical Silicon Carbide Converter (CVD Tungsten As Deposited Emitter, Nickel Collector)

This converter has been on life test for 4260 hours at an emitter temperature of 1730 K or higher.

The performance has been stable during the entire test.

At 1750 K, the DC output current is  $6.6 \text{ A/cm}^2$  at 0.3

V. The life test will continue.

B. Converter No. 247: Two-Inch Diameter Hemispherical Silicon Carbide Converter (CVD Tungsten As Deposited Emitter, Nickel Collector)

This converter continued on life test at an emitter temperature of 1650 K. The performance and the physical appearance of the converter has remained unchanged. The converter has operated for more than 1700 hours, and the life test is continuing.

C. Two-Inch Diameter Torispherical Silicon Carbide Converter

A design for a torispherical silicon carbide converter has been completed. A cutaway sketch of the converter is shown in Figure 10. The length of the hot shell-emitter is 2 inches and the diameter is 2 inches. The active area of the emitter is  $26 \text{ cm}^2$ . The electrode spacing is set during construction and maintained during operation by a ceramic spacer. The vacuum-tight ceramic seal does not support or separate the electrodes and so it is under much less stress than in previous designs.

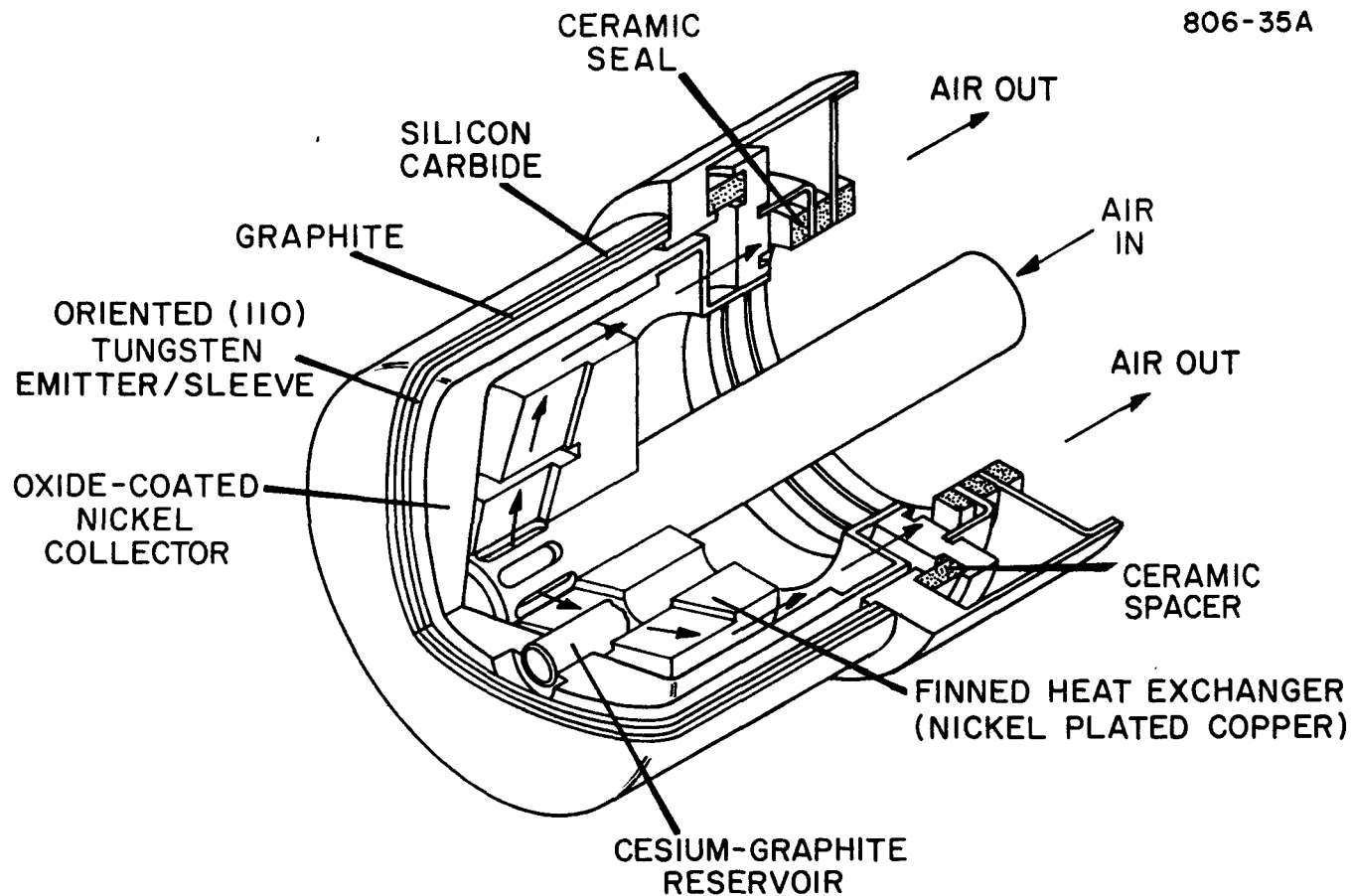


Figure 10. Two-Inch Torispherical Converter

The collector for the converter is made from nickel and cooled by a finned heat exchanger with two concentric rows having 18 and 36 fins. The collector can be coated with various oxides. The design also allows for either a liquid cesium reservoir or a cesium-graphite reservoir.

D. CVD Silicon Carbide Converter Module (Converter Nos. 250, 251, 252, and 253)

Construction of the four diode array has been completed, and testing has begun. A sketch of the module fixture with the four diodes in place is shown in Figure 11. Initially, all diodes will be optimized at an emitter temperature of 1600 K. After the optimization, the module will be operated as a unit. DC performance measurements as well as startup and shutdown characteristics will be measured.

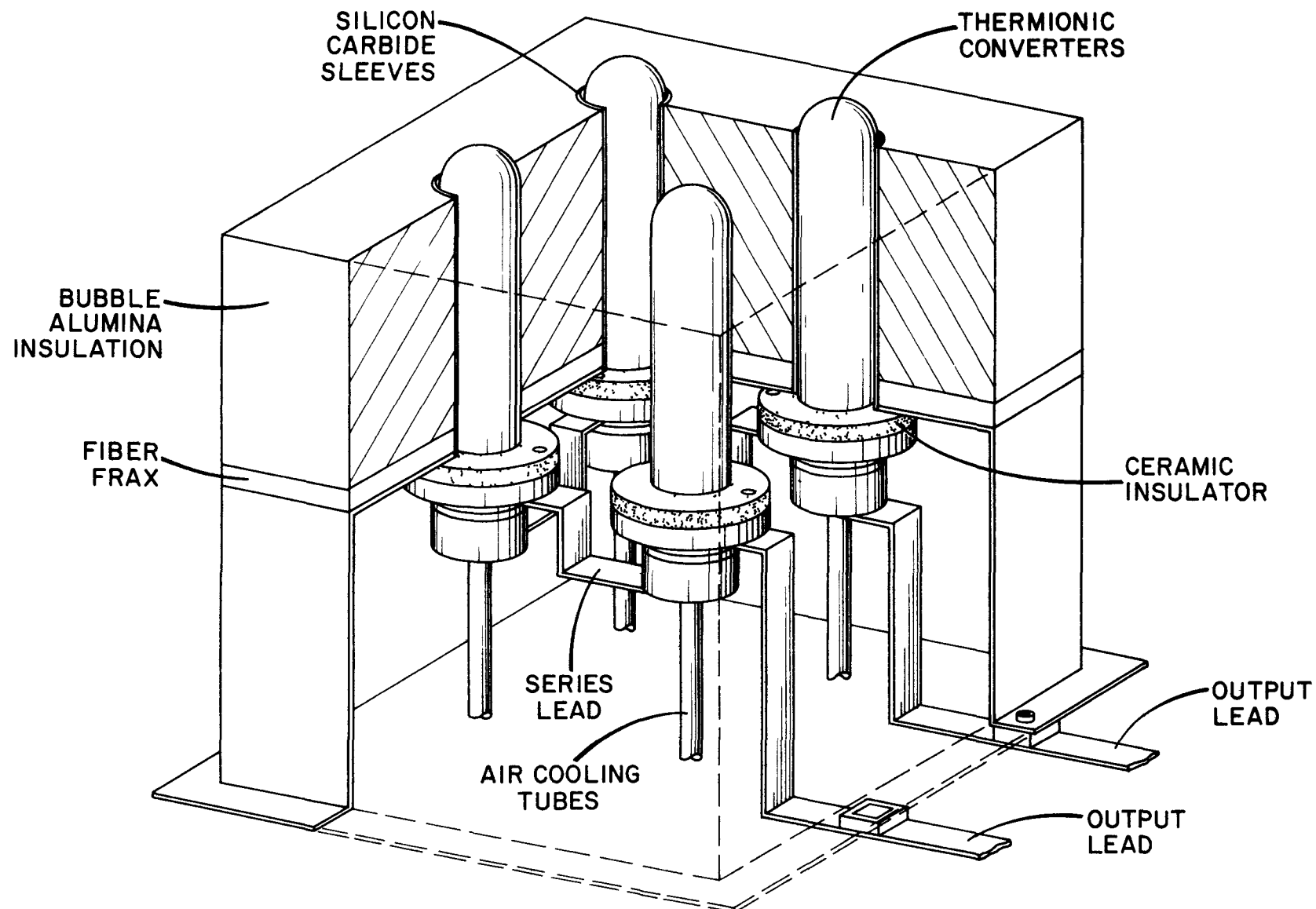


Figure 11. Four-Converter Array

### 1.2.3 TASK VII. COAL-FIRED TAM TEST UNIT

The objective of this task is to prepare plans for a TAM coal-fired test unit. The preliminary design will be formulated by taking into consideration the results of the system studies and TAM module development. The TAM test unit design will be the smallest size consistent with a realistic simulation of the temperatures, heat fluxes and slag conditions of a coal-fired steam powerplant.

Topical Report No. TE 4258-81-81, Coal-Fired Furnaces for Testing of Thermionic Converters, has been written and distributed. This report discusses the design costs of a facility, which adapts a coal-fired furnace built by Foster-Wheeler Development Corporation for thermionic converter testing. The arrangement of such a test furnace is illustrated in Figure 12. A facility of this type would be exempt from air pollution regulations because of its low firing rate.

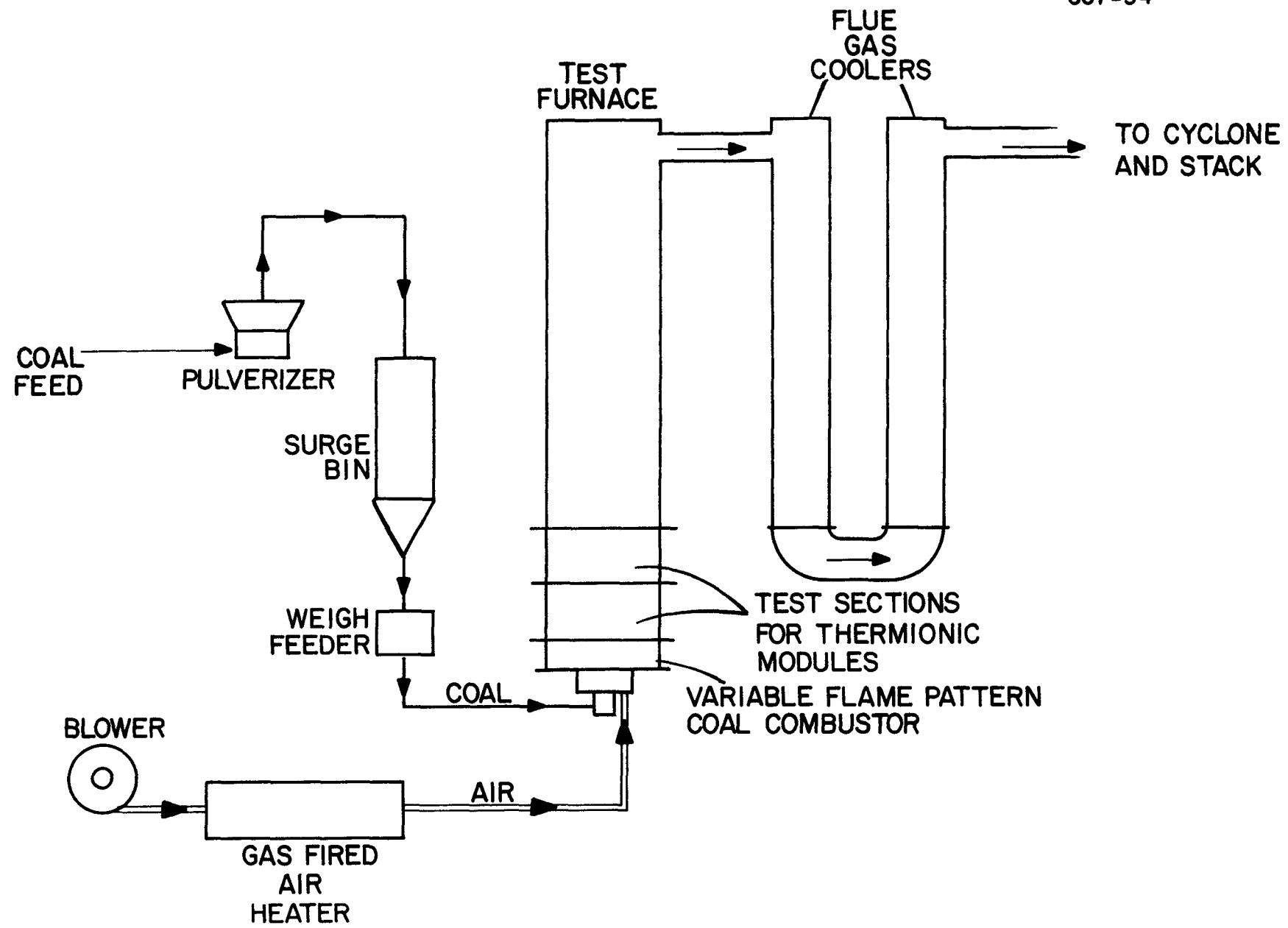


Figure 12. Schematic Arrangement of Test Furnace



## 2.0 PART TWO: NASA-OAST/JPL TASKS

### 2.1 THERMIONIC CONVERTER EVALUATION

#### 2.1.1 TASK VIII. HIGH-TEMPERATURE CONVERTER EVALUATION

The objective of this task is to characterize the performance of candidate emitters, collectors and converter configurations at the high collector temperatures (900-1100 K) required for nuclear electric propulsion. Variable-spaced, planar converters will be used for this task. Evaluation of each converter will include measurements of the output current density versus load voltage as a function of emitter temperature, collector temperature, interelectrode spacing and cesium pressure.

##### A. Converter No. 240 (JPL No. 10): Tungsten Emitter, Molybdenum Oxide Collector

The performance history of this converter was detailed in the previous progress report. A sudden increase in barrier index such as this diode experienced is occasionally explained by a leak contaminating the electrodes. The converter was taken off test and leak-checked through the cesium reservoir tubulation. No leak was found.

A second explanation put forward was that the oxygen reservoir in the collector had been depleted. To address this possibility, the collector was analyzed for oxygen content. It was found that the coating contained 2,180 ppm oxygen by weight. The control surface, which was sublimed at the same time contained 1,800 ppm oxygen. The two measurements are equal within experimental error. It is therefore assumed that the 100 hours of operation of this converter did not substantially deplete the oxygen source.

B. Converter No. 242 (JPL No. 9): Tungsten Emitter, Molybdenum Oxide Collector

The performance characteristics of this diode were given in the previous progress report. During this reporting period, the converter was placed in an ion pumped life test station in order to evaluate the long-term stability of the electrode pair. The diode is at operating temperature and current-voltage characteristics have been measured. A 0.1-ohm leakage path between the electrodes has been measured.

At this time, it is undetermined whether the short is in the interelectrode region or external to the diode. The vacuum system will be opened to examine the situation.

C. Converter No. 249 (JPL No. 15): Tungsten Emitter,  
Molybdenum Oxide Collector

The emitter of this converter is made from a chemical vapor deposition of tungsten. The surface was electroetched to expose 110 facets. The sublimed molybdenum oxide collector contained 9,880 ppm oxygen by weight.

Converters containing molybdenum oxide collectors tend to start out slowly. This diode was no exception. Initial current-voltage characteristics were resistive, and relatively high cesium pressures were required to obtain appreciable emission from the emitter. Unlike the previous molybdenum oxide diodes, the performance improvements, generally attributed to the collector, were gradual. The output improved to a barrier index of 2.06 eV, over a period of 60 hours. In all other aspects, this diode exhibited atavistic molybdenum oxide behavior.

The acquired data are presented as follows: Figure 13 is a typical cesium reservoir temperature family at  $T_E = 1650$  K,  $T_C = 750$  K and  $d = 0.50$  mm after 130 hours of operation; Figure 14 is the optimized envelope at  $T_E = 1650$  K for various spacings; and Figure 15 is the collector work function plotted against the ratio  $T_C/T_R$ .

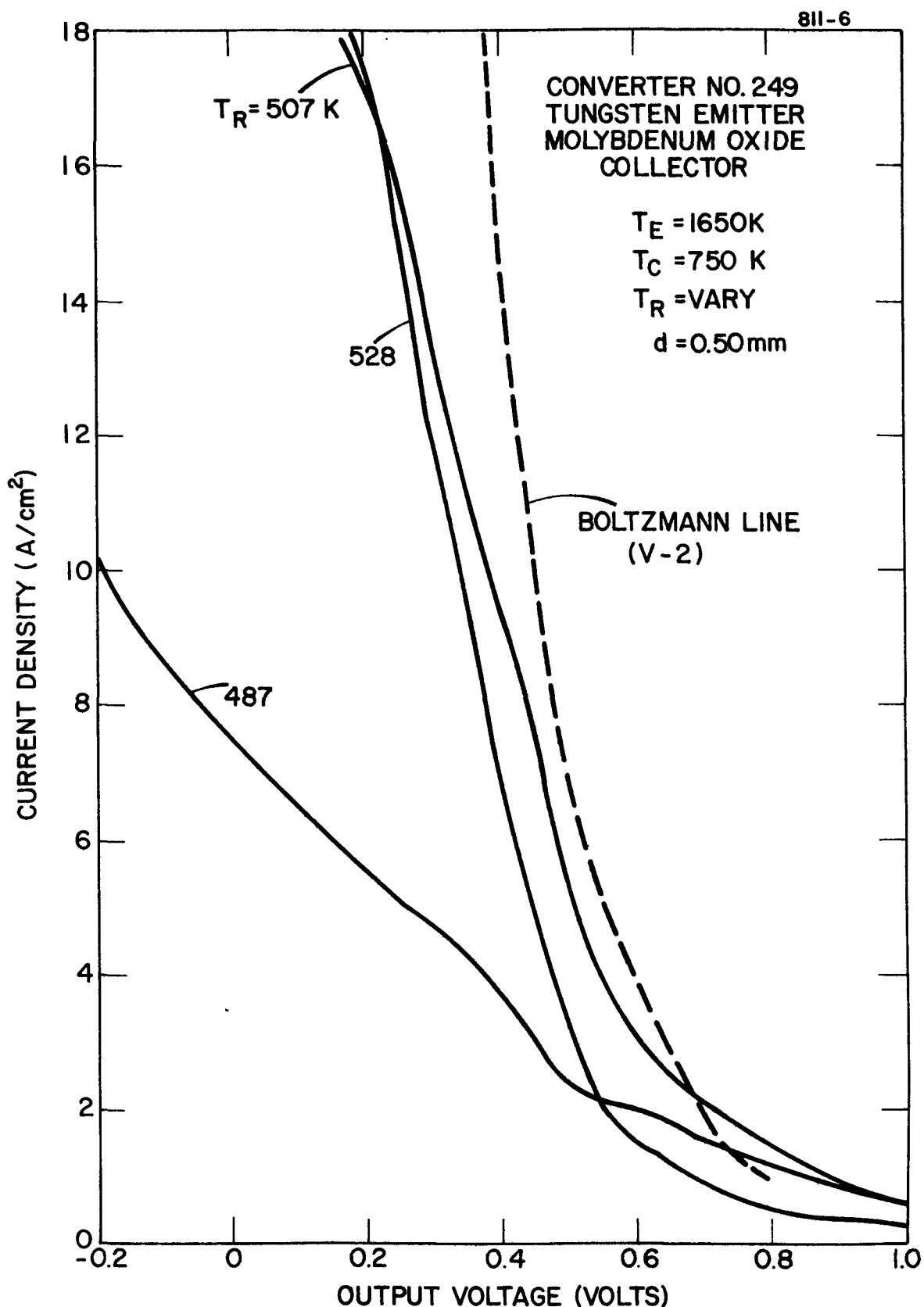


Figure 13. Cesium Reservoir Temperature Family for Converter No. 249  
 $(T_E = T_C = 750\text{ K} \text{ and } d = 0.50\text{ mm})$

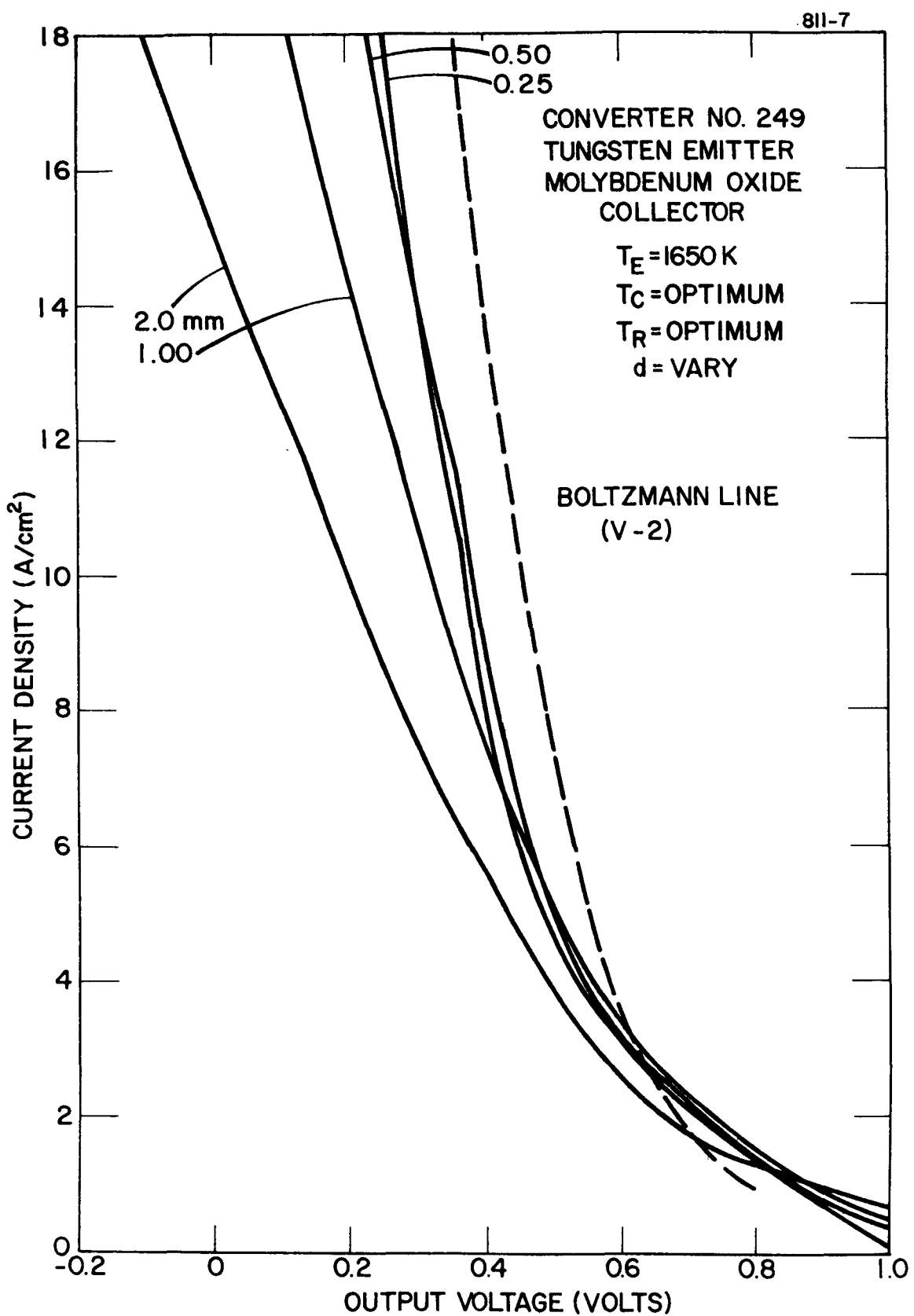


Figure 14. Optimized Converter Performance for Converter No. 249  
 at  $T_E = 1650\text{ K}$

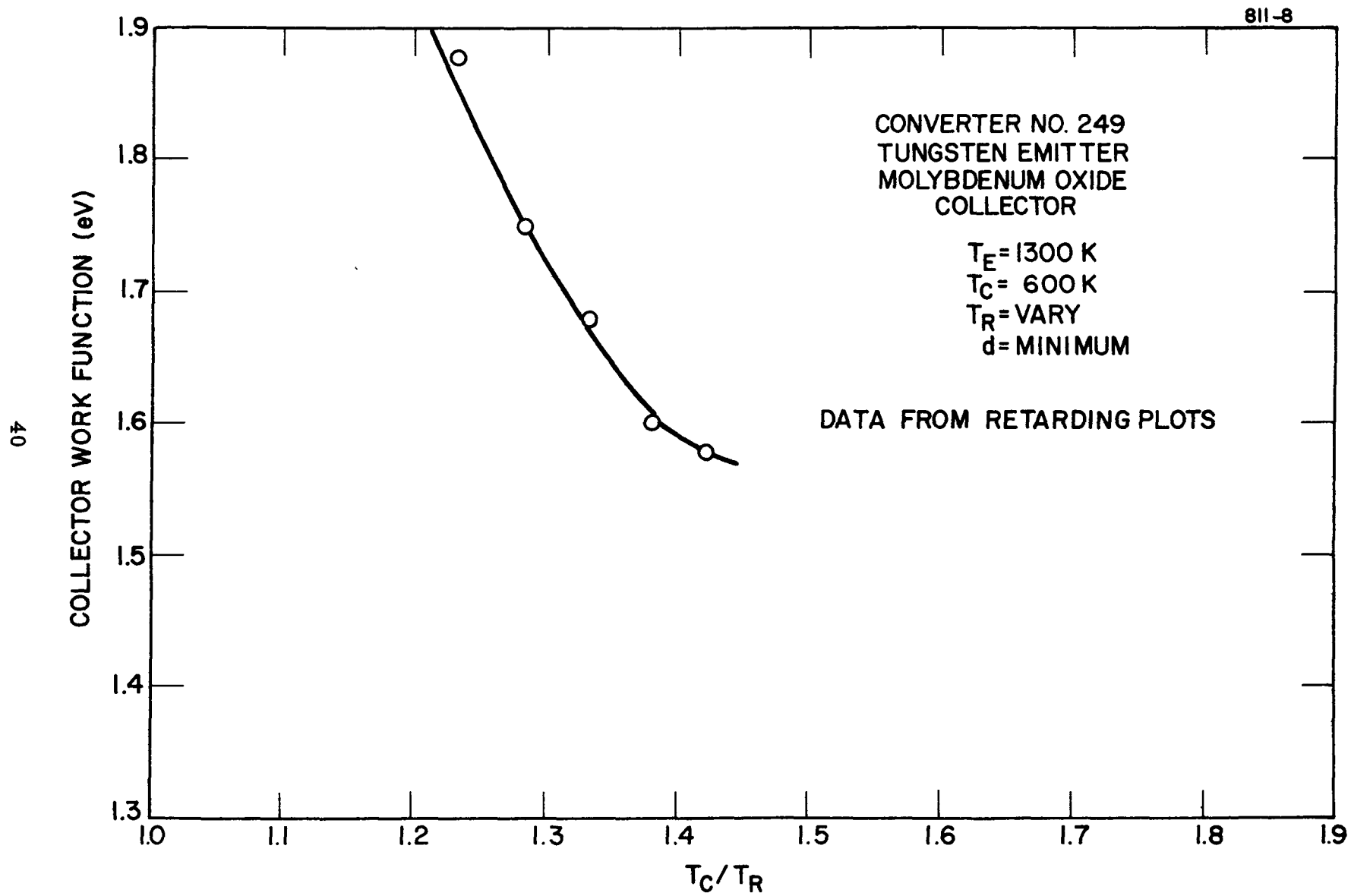


Figure 15. Collector Work Function Versus  $T_C/T_R$  for Converter No. 249

against the ratio  $T_C/T_R$ . The collector work function was measured by the retarding plot method. The minimum work function of 1.58 eV corresponds to a  $T_C/T_R$  of 1.42.

D. Converter No. 254 (JPL No. 14): Tungsten Emitter, Molybdenum Oxide Collector

This converter has an electroetched CVD tungsten emitter and a sublimed molybdenum oxide collector. The collector contains 9,880 ppm oxygen by weight. This collector is from the same sublimation run as that of Converter No. 249.

The performance history of this diode is very similiar to that of Converter No. 249. Initial curves were typical of young molybdenum oxide diodes, resistive and unoxygenated. Again the performance improved to a barrier index of 2.00 eV. This improvement took a period of 80 hours. Figure 16 is an example of a cesium reservoir temperature family at  $T_E = 1650$  K,  $T_C = 750$  K, and  $d = 1.00$  mm. The diode was optimized for cesium pressure and collector temperature at  $T_E = 1650$  K, the results are given, parametric in interelectrode spacing, in Figure 17. The collector work function was

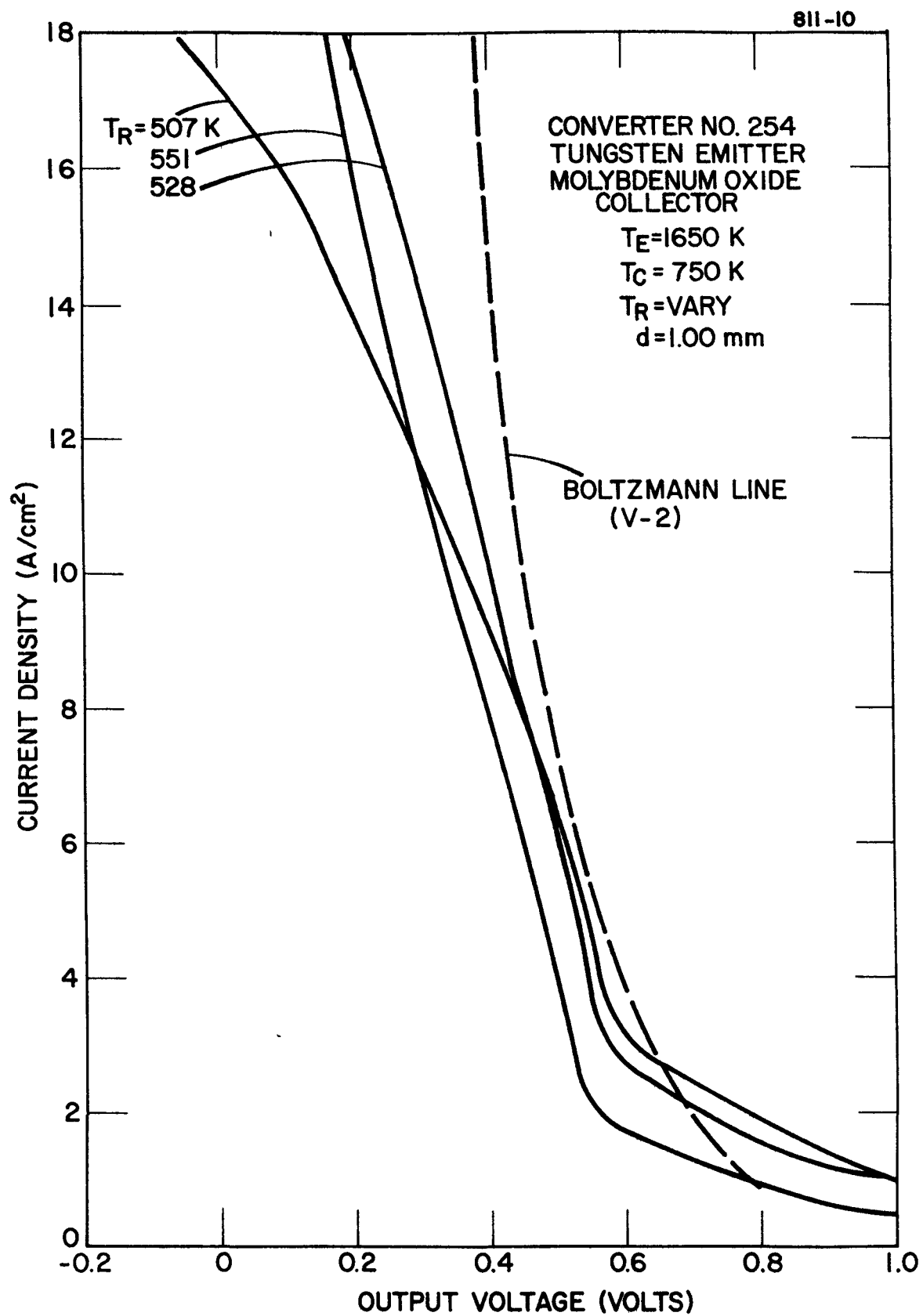


Figure 16. Cesium Reservoir Temperature Family for Converter No. 254  
 $(T_E = 1650$  K,  $T_C = 750$  K, and  $d = 1.00$  mm).

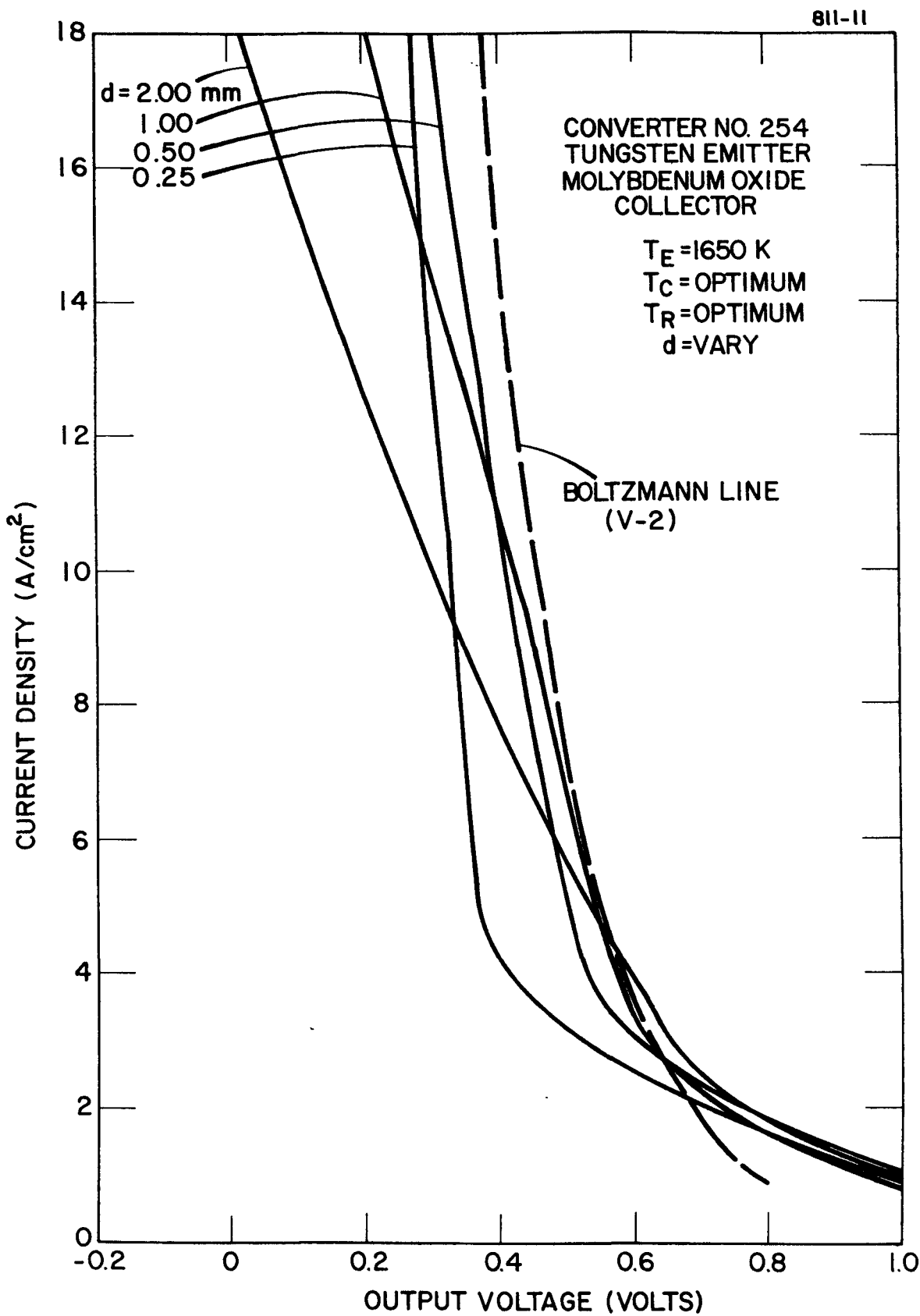


Figure 17. Optimized Converter Performance for Converter No. 254  
 $(T_E = 1650$  K, Parametric in Interelectrode Spacing)

measured by the retarding plot method. The minimum work function of 1.48 eV corresponds to a  $T_C/T_R$  of 1.52. This result is presented in Figure 18. At this time, the diode has run for approximately 200 hours at the improved performance level.

E. Converter No. 256 (JPL No. 16): Tungsten Emitter, Molybdenum Oxide Collector

The emitter of this converter is electropolished CVD tungsten. The molybdenum oxide collector contains 12,300 ppm oxygen by weight. This collector is from the same sublimation run as that of Converter No. 257.

The converter has been operated for a period of 123 hours. A typical cesium reservoir temperature family at  $T_E = 1650$  K,  $T_C = 750$  K and  $d = 1.00$  mm is given in Figure 19. The type of output seen in this figure is characteristic of a molybdenum oxide diode in an early stage of activation. Output will be monitored in order to detect any enhancement in performance.

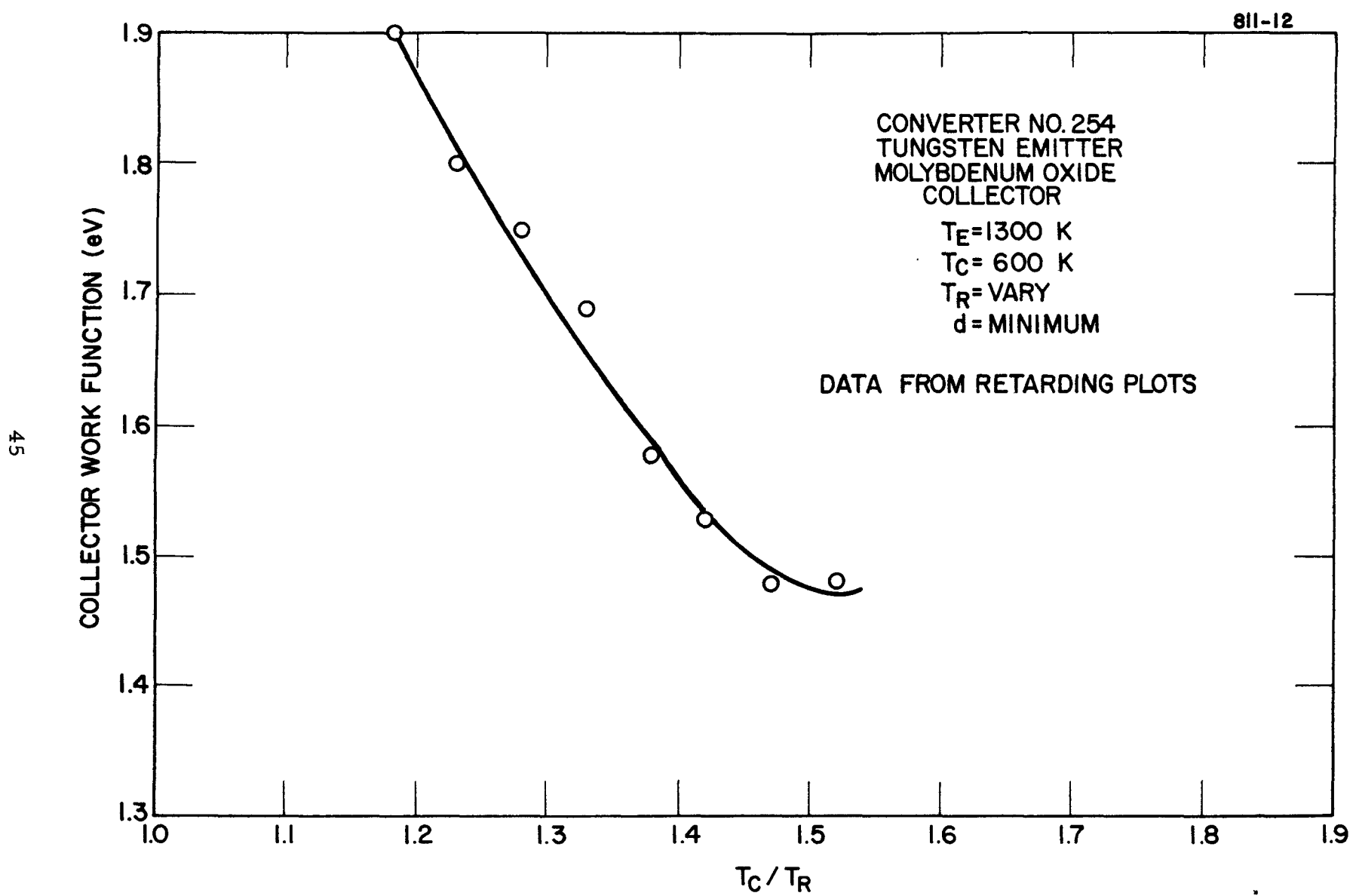


Figure 18. Collector Work Function Versus  $T_C / T_R$  for Converter No. 254

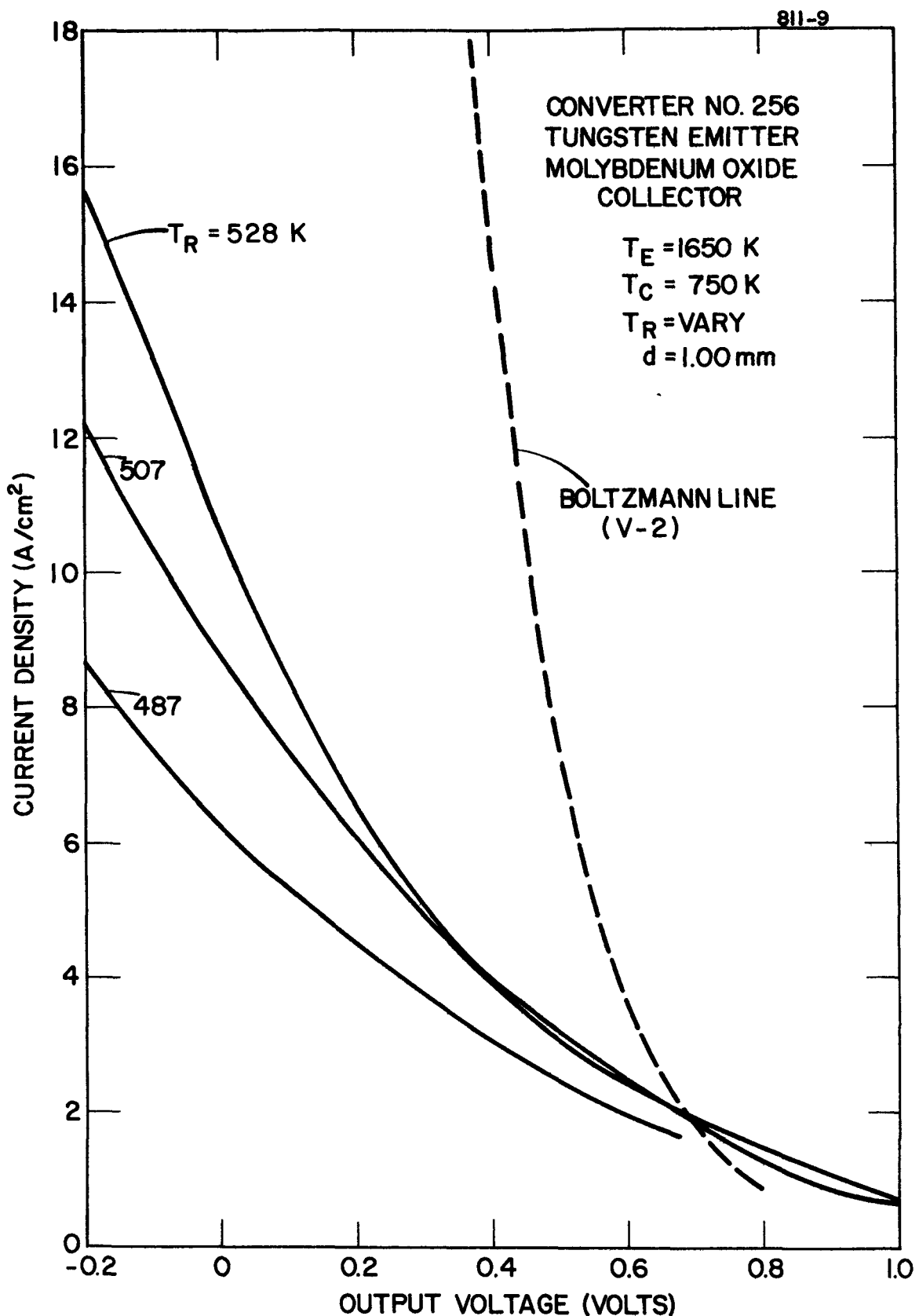


Figure 19. Cesium Reservoir Temperature Family for Converter No. 256  
 $(T_E = 1650 \text{ K}, T_C = 750 \text{ K}, \text{ and } d = 1.00 \text{ mm})$

F. Converter No. 257 (JPL No. 13): Molybdenum Emitter,  
Molybdenum Oxide Collector

Converter No. 257 has an electropolished molybdenum emitter and a sublimed molybdenum oxide collector. The control collector of this series contained 12,300 ppm oxygen by weight. The diode has been outgassed and cesiated, and testing has begun.

Initial current-voltage characteristics were resistive and exhibited a large barrier index. Figure 20 shows a cesium reservoir temperature family at  $T_E = 1650$  K,  $T_C = 750$  K and  $d = 0.50$  mm. Such characteristics are typical of early test data from converters containing molybdenum oxide collectors. As of this writing, the diode has operated at the foregoing conditions for a period of 72 hours. Apparently, cesium has not yet acted on the molybdenum oxide collector to produce a more electrically conductive surface. Testing will continue on this diode.

Due to program priorities established by JPL, no significant effort was expended on Tasks IX, X and XI during this reporting period.

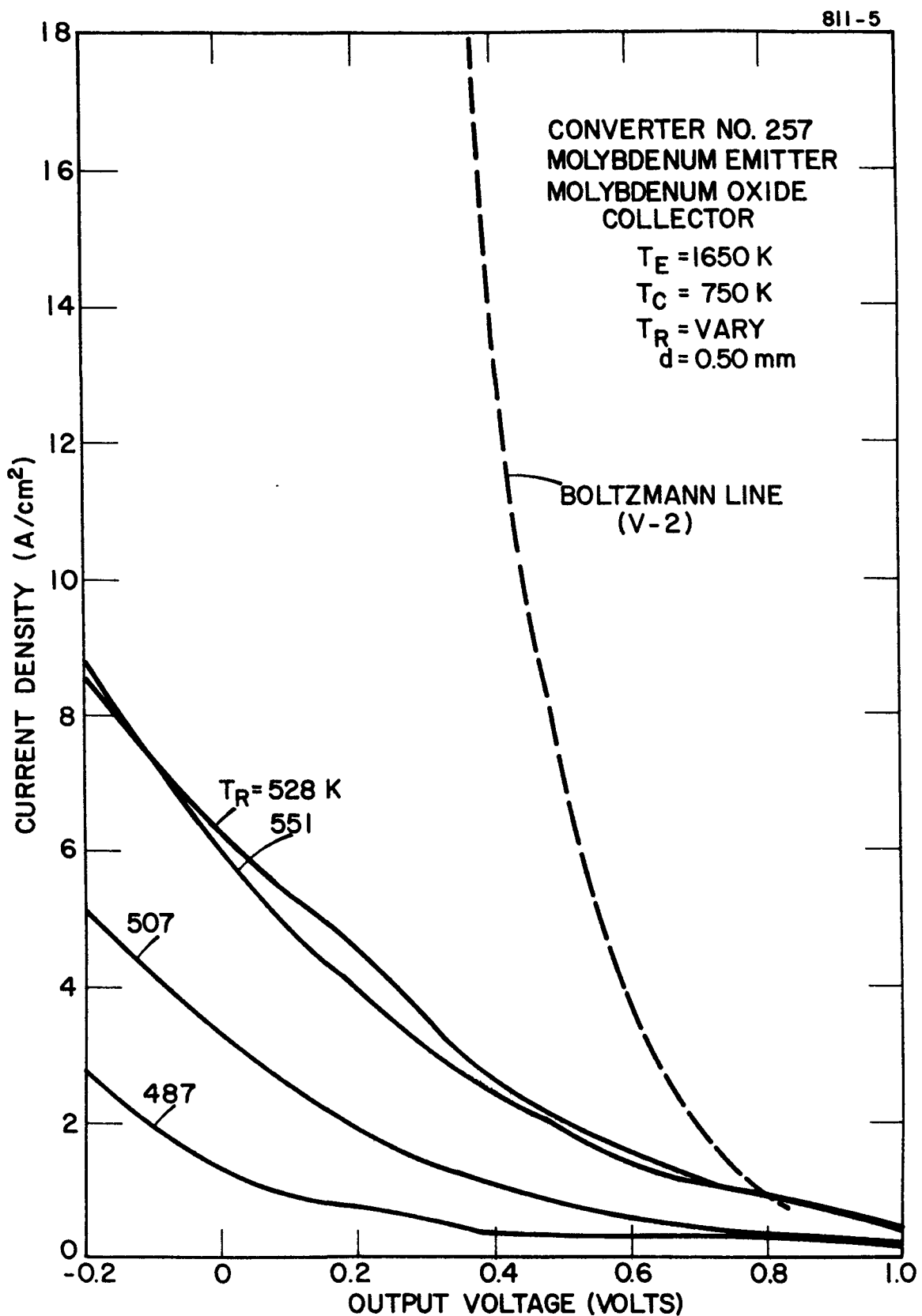


Figure 20. Cesium Reservoir Temperature Family for Converter No. 257  
 $(T_E = 1650 \text{ K}, T_C = 750 \text{ K}, \text{ and } d = 1.00 \text{ mm})$